University of Glasgow | School of Engineering

Thermal analysis of a novel space heating system based on thermo-geology

August 2014

A thesis submitted in partial fulfilment of the requirements for the degree of
MASTER OF SCIENCE IN SUSTAINABLE ENERGY

Abstract

This study was undertaken to complete an initial thermal analysis of a novel space heating system based on thermo-geology. This project focused on the addition and removal of heat from the earths subsoil, and its impact on the change in entropy and change in internal energy of the phases within the soil. The soil model presented was assumed to remain at thermal equilibrium throughout this study. As a result, the internal energy, and entropy were reduced to the calculated percentage contribution of the total change in the system.

From the investigation into internal energy, as heat was applied to the model, the vapour phase accounted for the majority of the total change in internal energy due to the latent heat of vaporization absorbed by the liquid undergoing phase change. This conclusion was also drawn for the total entropy change, where the level of disorder increased significantly as the liquid phase in the soil model moved into the vapour phase. In contrast, the study into the phase change as heat was removed from the soil model indicated that a significant decrease in entropy and internal energy of the solid water phase occurred, specifically as a result of the significant latent heat released by the liquid water phase on entering the solid phase.

This study goes on to investigate the effect of humidity on the variation in internal energy and entropy of the model, drawing the conclusions that as VPD decreases with humidity, the phase change within the model reduced as a consequence. The model presented was used to show that though the average specific heat capacity of the model increases, the overall heat required and therefore entropy change, and internal energy of the model reduces. The conclusion drawn is that a soil with a high relative humidity will require significantly less heat input to change the temperature of the soil. This indicates that using the soil as a heat reservoir for a space heating system would be most effective where the phase change in the soil could be controlled as a function of the humidity.

List of Objectives

General objectives

- Thermal analysis of a novel space heating system based on thermo-geology

Specific Objectives

- To learn about thermo-geology and its potential use within the global heat budget
- Understand the thermodynamics at work in the Earths subsurface
- Create a soil model based upon homogeneous thermal equilibrium
- Complete a study into the effects of heat transfer within the soil model

Thermo-geology is the study of the ground sourced heat and its potential application as a means of reducing the global heat budget. Ground sourced heat occurs in the shallow earth subsurface as a result of the heat flux from the sun that can be absorbed and stored in the soil.

The aim of this research is to investigate heat transfer within the earths subsurface and to gain a deeper understanding of this relatively new science. Currently the world depends on a significant amount of energy for both heating and power requirements. Thermo-geology has the potential to provide a significant amount of renewable heat to reduce the worlds power demands, and as a result, reduce out dependence on fossil fuels world wide.

In order to complete this study, a detailed investigation into the thermodynamics of the earths subsurface will be carried out, in an effort to enhance the understanding and potential implementation of this new science.

Acknowledgments

I would like express my thanks towards my mentor, and advisor, for giving me the opportunity to study this incredibly interesting new subject. I would also like to thank him for the many meetings we had and the guidance he provided on numerous occasions.

I would also like to take this opportunity to thank my fellow Masters students, who were always around whenever I needed a helping hand.

Nomenclature

A = area of evaporating puddle

C_p = specific heat capacity at constant pressure

C_v = specific heat capacity at constant volume

E = Evaporation rate

E_a = Actual Vapour Pressure

E_s = Saturation Vapour Pressure

H = humidity

J = Joules

K_m = Mass transfer coefficient

m = mass

MW = molecular weight

P = Pressure

Q = heat

R = Universal gas constant

S = Entropy

ΔS = Entropy Change

T = Temperature

ΔU = Internal Energy

ΔV = Volume change

x = mass fraction

Table of Contents

1. Introduction

1.1 Background

The Global Energy Crisis

Across the world, people are becoming more and more aware of the issues associated with heating from natural gas, and from other fossil fuels. The potential implications of the release of CO_2 and other greenhouse gases have been well publicized - yet to this day there has not been widespread changes to the carbon based economy within the UK and worldwide. The impacts of global warming are likely to be disastrous this century, with weather patterns changing worldwide including Tsunamis, Hurricanes as well as widespread flooding and drought across most corners of the globe.

It is therefore imperative at this time that the world focuses on efforts to find alternative, sustainable methods not only of power generation, but also of space heating and cooling for buildings to reduce the amount of CO_2 released into the atmosphere. One such alternative solution that is available is the use of heat pumps, which are known to harness the heat stored in the subsurface of the Earth to generate heat to be used in households and commercial buildings with a much lower environmental impact that conventional gas heating. [1]

Harnessing the energy of the Earths subsurface

The specific heat capacity is a unit used to describe the ability of a medium to store heat for each degree Kelvin. As the sun warms the Earth using infrared rays in the summer, the subsurface is able to store a large amount of the heat within the rocks and soils. The rock type varies depending on the particular position of the subsurface in questions, however the thermal conductivities vary from 0.3 W m^{-1} K^{-1} for coal up to 7.5 W m^{-1} K^{-1} for quartzite. [2] The specific heat capacity is a measure of the ability of a medium to store heat, per degree K; therefore a rock type with a high specific heat capacity indicates it has a high capacity to store heat. In the colder months of the year, it is therefore possible to extract the heat stored in the subsurface with the use of a heat pump, which can drive the temperature of the rocks up the temperature gradient to be used in the buildings on the surface of the planet.

The ambient temperature of the rock can be harnessed as a result of the hydrology typically associated with the subsurface. The subsurface of the Earth contains groundwater (with a specific heat capacity of around 4.188 kJ (kg K)$^{-1}$) which in the UK varies between 7 – 15^{0}C at a depth of 100m. The ambient temperature of the UK is transmitted through the ground at a thermal diffusivity of around 0.05m^2 day^{-1} resulting in an increase of temperature of 2.6^{0}C per 100m of soil. [3]

In Great Britain there are many different types of space heating systems, and the most common systems are indicated below in Table 1.

Heating System Used	Temperature of water supply (^{0}C)
Conventional hot water	60+
Modern low temperature	45-55
Underfloor waterborne	30-45
Warm air circulation	25-30

Table 1: Variation in temperature input for heating systems [4]

The most inefficient of these systems is clearly conventional hot water, with energy requirements to supply hot water at over 60^{0}C. Considering the average room temperature of the UK of around 24^{0}C, a building with poor insulation will dissipate a lot of that heat to the surroundings. From Table 1 it can also be deduced that the temperature of groundwater is far too low to provide a direct heat supply straight into properties on the surface. Therefore, to increase the temperature supplied to the buildings, a compression cycle is required, most likely in the form of a heat pump.

The Heat Pump

A water pump is designed to take water from a position of low head, to a position of high head by carrying out work, (e.g. electrical, mechanical.) In the same way a heat pump is designed with the sole aim of carrying heat from an area of high temperature, to an area of low temperature – the opposite direction a natural temperature gradient would occur, which again requires work to be successful. The diagram below, Figure 1, shows the working parts of a heat pump.

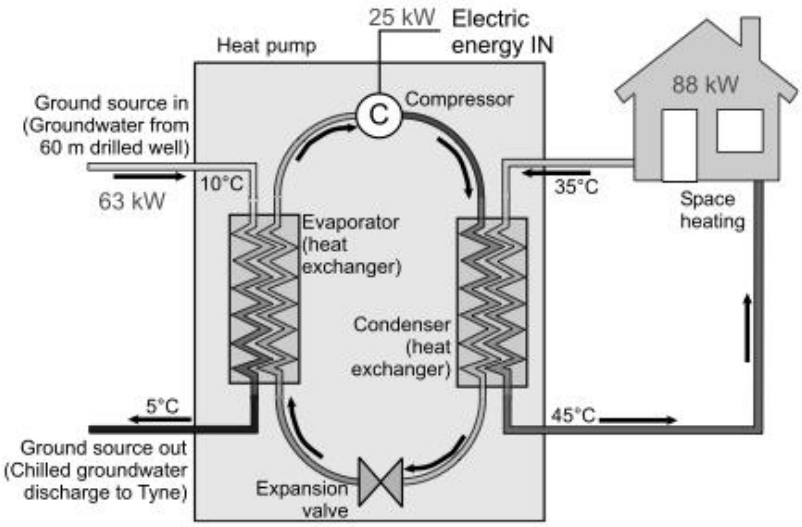

Figure 1: The implementation of a heat pump system [4]

Firstly, for a Ground Sourced Heat Pump (GSHP) to work it must have a borehole drilled to access the groundwater supply. Via a heat exchanger, the groundwater (7-15^{0}C) will exchange its heat with a refrigerant capable of transforming into a gas, and so absorbing latent heat from the groundwater when they exchange heat. The refrigerant gas is then passed through a compressor, which raises its pressure and so increases its temperature, as predicted by Boyle's law.[5] The high temperature gas can then be used in a central heating system to provide space heating for buildings. The gas is then passed through an expansion cycle, which causes it to condense, releasing its remaining heat, and the liquid refrigerant then completes the cycle by returning to the groundwater to be vaporized. Within the system the only electricity required is supplied to the compressor, considerably reducing the power required for the system and therefore the CO_2 emissions from generation.

A typical heat pump in the UK is a large investment, costing between £11,000 - £15,000 for complete installation of the heat pump, therefore it is extremely important to ensure that the system is designed to ensure maximum efficiency.[1] The smaller the temperature difference between the groundwater supply and the central heating network, the more efficient the heat pump will be. To measure the efficiency of the heat pump network, the coefficient of performance is used (Equation 1).[6]

$$COP_H = \frac{H}{W} \quad (1)$$

The coefficient of performance is useful when describing the basic efficiency of a heat pump system, however, since the efficiency of a heat pump varies due to a number of environmental conditions (e.g. delivery temperature and water inlet temperature), the coefficient of performance is not a fixed number, but will vary from day to day depending on subsurface temperatures and so will vary from season to season. For a typical ground sourced heat pump it is expected that the coefficient of performance will be have a minimum value of around 3. This means that for every 1 kW of electrical energy required, 3 kW of heat will be generated. This level of efficiency is the reason that GSHP's are so attractive, however the high capital costs of the installation means the level of uptake are relatively low except in areas where conventional gas and electricity are unavailable.

However with climate change continuing unabated, low energy space heating is one of the biggest requirements of the coming years. It is therefore important to model the subsoil effectively to maximize and utilize the renewable heat available from the Earth.

The chemical equilibrium of the subsurface of the Earth

Within the subsurface of the Earth there are a number of phases of state. Contained within the soil and the rock water will be present as a solid within the structure of soil itself, trapped alongside molecules of air, and between clay and mineral particles. Along with that there will be channels of water able to run as a liquid, as well as water vapour and gas present throughout the system. Therefore, to be able to model the soil as accurately as possible, it is important to have a complete understanding of the principles of chemical equilibrium associated with this system. At equilibrium we can use measureable qualities in thermodynamics to investigate how the phases of the Earths subsurface interact with one another, it is these quantities that will be utilized in this project in an effort to model unsaturated soils.

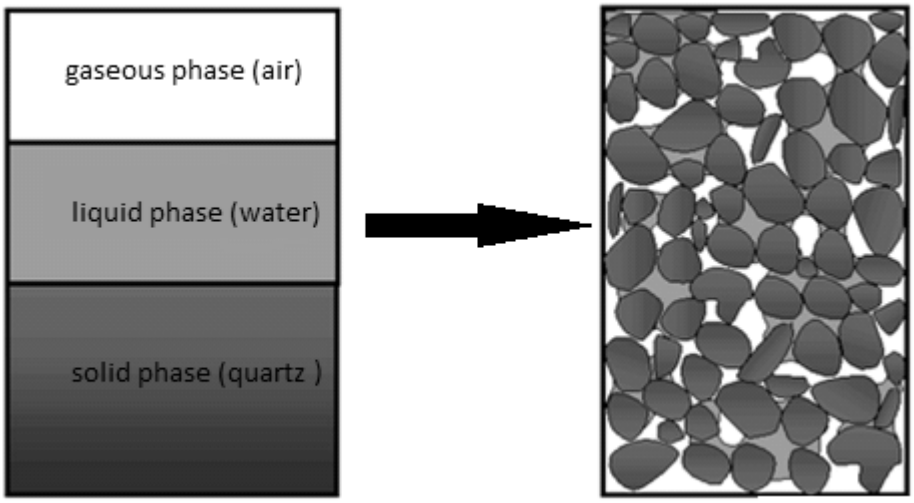

Figure 2: Three phase model of the soil

The diagram above indicates the soil model that will be presented within this study. A three phase model based on 25% air, 25 % liquid (water), and 50% solid (quartz). Typically less than 5% of the total soil tends to come from organic matter such as living materials, and decomposing plant litter, therefore these were omitted from this study. [7]

1.2 Outline

Section 1 of this project discusses the problems affecting the world's energy supplies and a potential solution to the global energy crises in the form of thermo-geology, along with its potential implementation using ground sourced heat pumps. The soil model to be investigated within this project is then introduced as well as the concept of chemical equilibrium within the subsurface of the earth and its importance to this study.

Section 2 discusses the theoretical background behind this project, introducing the method of investigating phase change within the soil, before discussing the effects this will have on the average specific heat capacity of the soil. Furthermore, the impact of humidity on the phase change within the soil is discussed, and its effects on the heat capacity. Section 2 continues to discuss the theory behind internal energy change and entropy change as heat is applied or removed from the model at thermal equilibrium.

Section 3 presents the results and discussion from all the investigations in this project. Initially the results from the study into phase change within the soil model is presented and discussed. Continuing to detail the results from the studies into the variation in entropy and internal energy of the soil model as heat is added. The results from the investigation into the removal of heat from the soil are then given, and the impact upon phase composition of the ice are given and discussed. Finally a study is carried out into the impact of humidity upon the soil model, and the subsequent variation in entropy change and internal energy change within the soil are given, along with the implications of the study.

Section 4 provides the main conclusions of this project.

Finally, the data used within this project to provide the final results of this project are given in the Appendices. Appendix A presents the data used to calculate the phase change within the soil. Appendix B shows the variation in specific heat capacity of this study. Appendices C and D provide the data used in the investigation into the variation in entropy and internal energy of the soil model as heat is added. Appendix E presents the data used to calculate the variation in entropy and internal energy of the soil model as heat is removed from it, and Appendix F provides the data used to calculate the impact upon entropy and internal energy of the soil model due to the impact of humidity.

2. Theory

For a process to be described as being at thermal equilibrium it must obey the zeroth law of thermodynamics.[8] That is that "If body A is in thermal equilibrium with body B, and that body B is in thermal equilibrium with body C, then body A is in thermal equilibrium with body C.[9] For any multi component system, given enough time and treated as an isolated closed system, the system itself will reach internal thermal equilibrium.[10]

In this thermal analysis of a homogeneous soil model, it is assumed that the system obeys thermal equilibrium throughout. By assuming that the process is adiabatic, the zeroth law will apply, indicating that any heat added to the system will result in a homogenous increase in temperature across the soil model – irrelevant of the corresponding phase composition within.

Within this study, each component within the soil is treated as being in thermal equilibrium with each of the other components, allowing a detailed analysis of the entropy change within the model, as well as the variation in internal energy within the model from the original state at T = 283 K. This temperature relates to a common earth subsoil temperature in the UK. [11] The unsaturated soil model investigated throughout this study is based upon a commonly used 3-phase model at an initial state comprising of 50% solid (silica/quartz) phase, 25% gaseous (air) phase and a 25% liquid (water) phase at the initial temperature of the study.

2.1 The Relationship between heat added and specific heat capacity of the soil

Assuming thermal equilibrium within the soil model allows the heat added to the system to be directly related to the absolute temperature (T), of the model, as a function of the average specific heat capacity of the soil. [12]

$$cp\ av\ \equiv \frac{Q}{T} \tag{2}$$

The average heat capacity of an isolated, unsaturated soil can therefore be measured by knowing the heat put into the system and assuming it is a closed system, i.e. that all heat is transferred internally in the soil model, as well as having the capability to measure the

temperature change within the soil. When modelling the interaction between different phases within an unsaturated soil system, the average specific heat capacity of the soil will be an important tool to distinguish between the physical characteristics of the soil model presented. The average specific heat capacity can then be calculated as a function of the mass fraction and the specific heat capacity of each component within the soil model.

Throughout the study of this soil model, the heat applied to the soil will be provided at the same rate (42 kW) selected due to its common implementation as the power output of a heat pump. To calculate the average heat capacity of the soil at a series of different temperatures, an understanding of the phase change within the soil was required.

2.2 Phase change within the soil model

To carry out a complete thermal analysis of this homogeneous soil system it was of fundamental importance to investigate how the composition of the individual phases within the soil model change as temperature is increased. As the composition of the soil changes, the thermal relationships within the study will also vary. Therefore, in an effort to carry out this study accurately, an investigation into the composition change occurring in the soil has to be completed.

This includes investigations into;

- the Vapour Pressure Deficit as temperature changes,
- the evaporation rate within the soil model across the temperature range,
- the variation in heat capacity of the soil model,
- the heat required to raise the temperature within the soil model,
- the composition change of the soil with time.

2.2.1 Vapour Pressure Deficit (VPD)

Vapour Pressure Deficit (VPD) is measure of the difference between the saturation vapour pressure (E_s) and the actual vapour pressure (E_a) in a system. VPD can be viewed as a measure of the ease at which evaporation within the soil under certain conditions can occur. VPD can

be calculated using the Antoine's equation to calculate the saturation vapour pressure, before using humidity to calculate E_a. [13]

$$E_S = e^{(A-\frac{B}{C+T})} \quad (3)$$

Where *A*, *B*, and *C* are material specific coefficients. For water, A =8.07131, B = 1730.63, C = 233.426, too give Es in mmHg. [14] *T* is the temperature at which the saturation vapour pressure is required. The actual vapour pressure can then be calculated multiplying the saturation vapour pressure (E_s) by the humidity (H), before VPD is calculated.

$$E_a = E_s \,.\, H \quad (4)$$

$$VPD = E_s - E_a \quad (5)$$

2.2.2 Evaporation Rate in the Soil

To investigate the phase change within the soil, a realistic potential evaporation rate within the soil was required. The Penman-Monteith equation for evapotranspiration, first published in 1969, has been presented as a method used to calculate a rate of crop water requirements in agriculture.[15] The data intensive nature of the Penman-Monteith method to calculate evapotranspiration rate, particularly for the advective term which was identified by Saxton in 1975 as being the less dominant term in the combination equation, indicated that the use of this equation would have resulted in an inaccurate calculation of the phase change within this study.[16-17] In 1972, an investigation into the application of the Penman-Montieth equation was carried out by Priestly and Taylor. They discovered that the potential evaporation rate calculated using the Penman-Monteith equation was consistently 1.26 times lower than the actual value. In their modification of the Penman-Monteith equation, the advective term, calculated based on wind conditions above the soil, was removed and replaced by the term the Priestly-Taylor coefficient.[18] The Priestly-Taylor equation is therefore commonly used in sites where wind data in unavailable, however due to the incorporation of crop leaf index and net radiation term within the equation it was determined that the potential evaporation rate of the soil would be too unreasonable to use in a thermal analysis of the earths

subsurface. Therefore, within this study the estimated evaporation rate was calculated using the method proposed by Kawamara and Mackay.[19]

$$E = A \,.\, Km \,.\, \frac{Mw.Pv}{R.T} \tag{6}$$

For this study it was assumed that A = 10 m^2, Km = 0.05 m s^{-1}. When compared with the evaporation rates at 0% humidity calculated by the Priestly-Taylor method, these assumptions related the evaporation rates most closely.

To investigate the effect of humidity on the evaporation rate calculated within the soil, the vapour pressure calculated within the soil was replaced by the VPD previously calculated in this study to show the direct correlation between humidity upon the calculated evaporation rate. The effect of humidity on phase change within the soil can then be investigated by basing the vapour pressure on VPD, a function directly related to humidity (Equation 5).

2.2.3 Study into the variation of heat capacity of the soil model

Following the investigation into the evaporation rate within the soil, the variation in specific heat capacity can then be modelled as a function of time due to the dynamic phase change calculated. Assuming a homogeneous soil, at thermodynamic equilibrium, it is then possible to use the average specific heat capacity of the soil as a measure of the dynamic phase change within this multi-phase system.

$$c_{p_{av}} = x_{solid} c_{p\ solid} + x_{liquid} c_{p\ liquid} + x_{gas} c_{p\ gas} + x_{vapour} c_{p\ vapour} \tag{7}$$

Using the mass fraction of each component (x_i) allows the average specific heat capacity to be calculated as a function of the percentage mass of the soil each phase represents. The study into average heat capacity provides data on how the increasing evaporation rate within the soil will have an impact on the average specific heat capacity of the soil.

The average specific heat capacity can then be used in a homogeneous system to calculate the heat required to bring about a definite temperature change within the soil, assuming no waste heat is lost to the surroundings in the closed thermodynamic environment.

Having calculated the average specific heat capacity of the soil at the initial temperature, the heat required by the homogeneous soil model to increase the overall temperature within the soil could be calculated.

To continue the thermal analysis of the multiphase soil system, the average heat capacity of the soil previously identified must now be applied to determine the actual heat required to raise the temperature of the soil. It was assumed that the specific heat capacity of the soil remained constant from the initial temperature, T_i to T_1, before the phase change within the soil at T_1 was calculated and then used to provide the specific heat capacity at T_1. Within this thermodynamic system it is assumed that there is no pressure change across the temperature range therefore the heat required to raise the temperature of the soil from T_i-T_1, can be calculated using the following equation.

$$Q = c_p m(\mathrm{T}_1 - \mathrm{T}_i) \tag{8}$$

Since the temperature change has already been selected and the heat pump had already been selected at 42 kW it is then possible to calculate the rate at which the temperature within the soil changed (K s^{-1}) at which the soil will heat up, based on the specific heat capacity.

$$\dot{\Delta T} = \frac{\dot{Q}}{cp_{av} m} \tag{9}$$

From Equation 17, it is then possible to calculate the actual heat required to raise the temperature of the soil based on the average specific heat capacity using Equation 10, below.

$$Q_{req} = \frac{\Delta T}{\dot{\Delta T}} . \dot{Q} \tag{10}$$

Having calculated the actual heat required to bring about the required temperature change in the soil, it is then possible to calculate the time taken for the soil to reach the required temperature since the heat pump supplies the heat at a given rate (42 kW).

$$t = \frac{Q}{\dot{Q}} \tag{11}$$

2.2.4 Total Phase Change

From the previous investigations into evaporation rate and the time taken for temperature change within the soil, it is then possible to analyse how the phase change within the soil takes place in the time calculated in Equation 11. By combining the evaporation rate (Equation 6) with the time taken, the total evaporation and therefore total phase change within the soil model can be calculated, thereby providing a realistic analysis of the impact of the rate of evaporation on the phase change within the soil.

$$E_{total} = t.\dot{E}_{mass} \tag{12}$$

At this stage it was assumed that no latent heat was required to be absorbed by the liquid phase within the soil to transition to the vapour phase. Since the evaporation rate was calculated in kg s^{-1}, this assumption allowed the estimated evaporation rate to determine the total phase change across the temperature range, whilst also allowing the increasing evaporation rate across the temperature range to be investigated during phase change analysis. For subsequent calculations into the determination of total heat required by the soil, the latent heat is included.

Having calculated the phase change of the water within the homogeneous soil model, the average specific heat capacity can then be modelled accurately across the temperature range. This allows internal energy, heat required and finally the total entropy change within the system to be investigated within this thermal analysis of a thermo-geological heating system.

2.3 Entropy Change within the unsaturated soil model

In a reversible process or in a uniform (homogenous) system, entropy is a conserved quantity and there will be no change in the overall entropy of the system. In contrast, in an irreversible process, the entropy change within a model as heat or temperature varies cannot be considered as being conserved, and based on the second law of thermodynamics, the entropy of the universe must increase. Focussing on a cyclic/reversible process the change in entropy

can be calculated as a function of the heat absorbed by the body, divided by the absolute temperature. [20]

$$\Delta S = \int \frac{\delta Q_{rev}}{T} \tag{13}$$

This equation has been described as one of the state functions within thermodynamics, with heat transfer taking place between two bodies the overall entropy change will be positive, as temperature is transferred from the hot body to the cold. This is in accordance with the 2nd law, which indicates that the entropy of the universe must not decrease, in this study, the assumption is that the entropy added or removed from the soil is part of heat pump cycle, and therefore will result in an equal or greater entropy change where the heat from the soil is being utilized. This can be seen as the quantity of heat absorbed by the cold body being equal to the quantity of heat lost by the hot body. [21]

$$\frac{\partial Q}{T_H} < \frac{\partial Q}{T_C} \therefore \partial S_{positive} \tag{14}$$

If a system is at thermal equilibrium, and the only process it undergoes is the addition or removal of heat, this will result in a change of state within the system and thereby result in a change in state, and thereby a definite change in the entropy within the system. At thermal equilibrium, the calculation of entropy reduces to the partial equation, shown below. [22]

$$dS = \frac{dQ}{T} \tag{15}$$

This equation is used throughout the thermal analysis of the unsaturated soil model presented, and can be used in the subsequent investigations into the variation in internal energy of the soil. When transitioning from the liquid phase to the vapour phase, the corresponding increase in disorder can be calculated using the Entropy of vaporization (ΔS_{vap} = 108.951 J mol^{-1}).[21] In the opposite direction, the decrease in entropy associated with the liquid phase moving into the solid phase can be calculated using the Entropy of fusion (ΔS_{fus} = -22 J mol^{-1}), the negative sign indicating the decrease in entropy across the phase change. [23]

2.4 Internal Energy of the soil model

The internal energy of a molecule is the summation of its translational, rotational, and vibrational energy. When the soil model state changes from $T_i \rightarrow T_1$, assuming heat is applied to the system, this will result in the internal energy of the molecules increasing as a function of the temperature. Within this study, for this unsaturated soil, it is assumed that the pressure in the soil remains at 1 atm throughout.[24]

$$\Delta U = T\Delta S - P\Delta V \tag{16}$$

$$T\Delta S = dQ \tag{17}$$

$$\therefore \Delta U = Q - P\Delta V \tag{18}$$

$$\Delta U = c_v . m . \Delta T - P . \Delta V \tag{19}$$

This equation holds true in a closed system where the only change to the system comes as a result of the addition or removal of heat within it. This equation can be used for liquids and solids, using c_v to calculate the increase in internal energy, while c_p is typically used for the calculation of heat requirements, and entropy change. Due to the small apparent volume change in the solids and liquids over the temperature ranges investigated in this study, PdV can be ignored. For a gas, the variation in internal energy can be calculated using the following equation, depending only on the ΔT of the system, as well as the number of moles of the gas.[25]

$$\Delta U = \int_{T1}^{T2} n . c_v . \delta T \tag{20}$$

Within this thermal analysis of the earths subsurface, both the air in the voids of the soil model, as well as the water vapour generated during the phase transitions within the model are treated as ideal.

For the phase transition between the liquid and the vapour phase, the latent heat of vaporization for water must be absorbed by the liquid phase before phase change will occur. Therefore, when calculating the total heat required in the study into the effect of humidity, the latent heat of vaporization is required since it accounts for a significant increase in the internal energy of the vapour phase, due to the size of the latent heat of vaporization for water (ΔH_{vap} = 2256 kJ/kg).[26] For the transition from the liquid phase into the solid phase,

the latent heat of fusion (334 J g^{-1}, 6.02 kJ mol^{-1}) is released by the liquid phase as it freezes. [26-27].

The total change in internal energy of the homogeneous soil model can then be calculated as a summation of the change in internal energy of each phase.

$$\Delta U_{total} = \Delta U_{solid\ phase} + \Delta U_{liquid\ phase} + \Delta U_{gas\ phase} \quad (21)$$

By investigating how the change in internal energy is stored within the individual phases in the soil model, it was then possible to calculate the proportion of the internal energy from each phase.

In 1967, D. Anderson investigated soil composition and gathered evidence indicating that in freezing conditions, there remained an unfrozen water content within the soil attached to the solid phase, between -5 and -10^{o}C. He estimated of that at -10^{o}C the unfrozen water content within the soil can be approximated to 0.3 g unfrozen water per gram Clay (MW = 258).[29] In this three phase model of the soil, the clay is replaced simply by quartz (MW = 60.01). As a result, the unfrozen water content per gram quartz is refined to = 0.0698 g. This ratio is used in the investigation into the heat removed from the soil, and its subsequent effects on the change in internal energy and entropy change within the homogeneous soil model.

Finally, the impact of humidity on entropy and internal energy within the model is studied based on the variation of phase change as a result of the decreasing vapour pressure deficit within the soil.

3. Results and Discussion

3.1 The investigation into the phase change within the soil

3.1.1 Vapour Pressure Deficit

Figure 3 shows the variation in VPD as humidity of the soil atmosphere increases.

The full range of data used to calculate the phase change within the soil is shown in Appendix A.

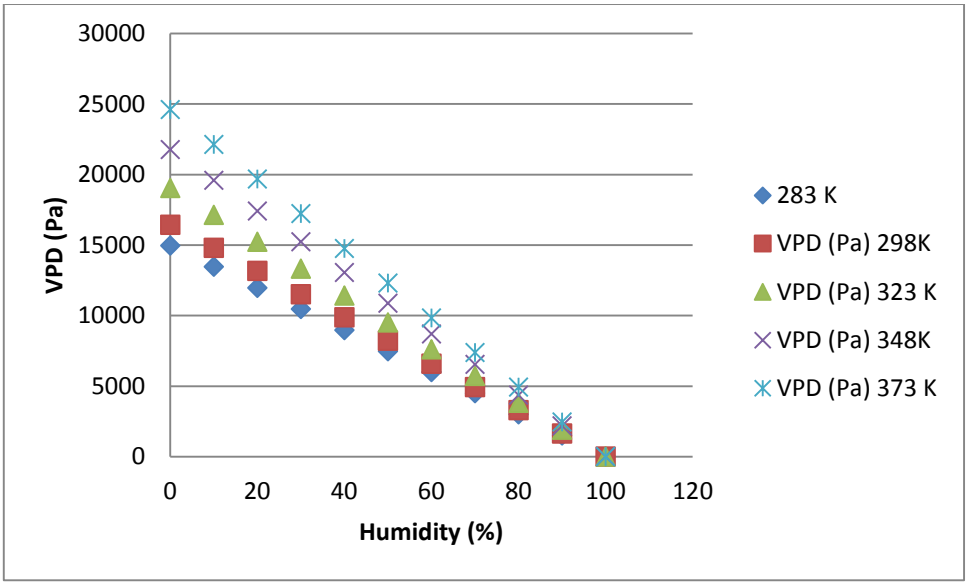

Figure 3: The variation in VPD as a function of humidity

The greatest variation in VPD occurs where the soil model reaches the highest temperature in this investigation (273 K), with the difference in VPD from 0 to 100 % humidity decreasing across the temperature range. Furthermore, as humidity increases the VPD within the soil can be seen to decrease to 0 Pa. Where the VPD reaches zero, it indicates that there is no opportunity for phase change to occur from liquid to vapour, as the air within the soil will have no capacity to hold any additional water vapour. It was anticipated that this would have a significant effect on the estimated evaporation rate.

3.1.2 The variation in Evaporation rate within the soil model

Using the formula proposed by Kawamara and Mackay, the evaporation rate can be calculated assuming an area of the evaporating puddle of 10 m^2, and a mass transfer coefficient of air in the soil of 0.05 m s^{-1}. The results of the investigation into the evaporation

rate within the soil are shown below in Figure 4, and the data used can be seen in Appendix A.

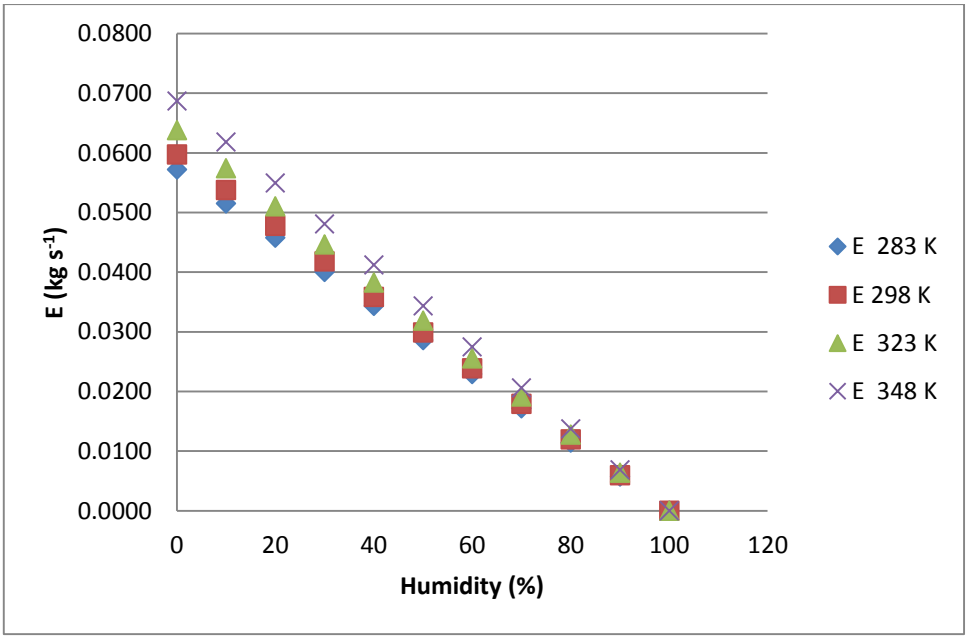

Figure 4: Variation in evaporation rate as a function of humidity

From the chart, the evaporation rate over the temperature range is seen to increase with temperature, due to the relationship between evaporation rate and vapour pressure. As the humidity of the soil model increases, the resulting decrease in vapour pressure deficit within the soil results in the estimated evaporation rate across the humidity range showing a linear downward trend before reaching 0 kg s^{-1} at 100 % humidity as the VPD tends to 0 Pa. This indicates that irrespective of the temperature within the soil model, as humidity increases the phase change of water to the vapour phase will, as anticipated, reduce to zero, and no phase change will occur. This will have a profound effect on the variation of heat capacity within the soil itself.

3.2 The variation of heat capacity within the soil

To continue the study into the thermal analysis of the soil model, the variation in heat capacity due to the rate of phase change within the soil model was investigated. The average heat capacity of the soil was calculated as a function of the mass fractions of components within the soil.

The composition of the vapour and liquid phases within this soil model will have the greatest impact on the average specific heat capacity of the soil. However, since heat capacity (both

c_p and c_v) will also vary simply as a function of temperature, this will also have an impact on the average specific heat capacity of the soil. The variation in specific heat capacity can be seen in Appendix B. Using the average specific heat capacity calculated from the initial thermal analysis of the soil at its initial temperature of 283 K, it was then possible to calculate the time taken to heat the soil to a given temperature based on a rate of heat being applied to the soil of 42 kW. It was assumed that there was no water vapour present in the soil at 283 K. The initial mass fractions of the composition of the soil model are available in Appendix B, and were selected as they are typical of a soil with ideal growing conditions (Figure 2). The total mass of the soil was set at 40 kg. For this study, the humidity was kept constant at 0%. The subsequent data required to calculate the rate of heat change in the soil and the total heat required across the temperature range can be found in Appendix B. Initially, the latent heat of vaporization was omitted from this study, instead the time taken for temperature change was based only on the specific heat capacity of the soil model.

Initial Temperature (K)	283
Delta T (K)	15
Rate of temperature change ($K\ s^{-1}$)	0.63
Heat Required (kJ)	994.3
Time taken (s)	23.67

Table 2: The heat required from 283 - 298 K

Initial T (K)	ΔT (K)	Initial Heat Capacity J $(kg\ K)^{-1}$	Evaporation rate $(kg\ s^{-1})$	time taken (s)	total time (s)	total phase change (xi)	total heat (kJ)
283	15	1657.2	0.057	23.67	23.67	0.034	994.3
298	25	1586.1	0.060	37.76	61.44	0.091	1586.1
323	25	1469.5	0.064	34.99	96.43	0.154	1469.5
348	25	1344.3	0.069	32.00	128.43	0.25	1344.3

Table 3: Results from the phase change at 0% humidity

From the results shown above, it can be observed that as the temperature of the soil model increases, the average specific heat capacity of the soil decreases. This correlation is as a result of the increased phase change from the liquid phase to the vapour phase within the soil. Since water in the liquid phase has a specific heat capacity of 4180 J /kg K at 25^{o}C, in comparison to the heat capacity of water in its vapour phase 1860 J/ kg K, this indicates that

for an equal mass of water vapour and liquid water, it would take significantly less energy to raise the temperature of the vapour. This is reflected in the reduction in the heat required to raise the temperature of the soil, from 1586 kJ required to raise the temperature from 298 – 323 K, reducing to 1345 kJ required for the transition between 348 – 373 K. The final specific heat capacity assuming total complete phase change within the liquid phase in the soil occurred at 373 K, with a value of 1138 J (kg K)$^{-1}$. As anticipated the time taken for the temperature change also follows a decreasing pattern, reducing by approximately 6 s from 298K (38 s) to 32 s in the final temperature transition. The values at 283 K appear to contradict this conclusion, however, this is due to the reduced ΔT during the first temperature transition, making them less valuable when observing trends.

The variation in specific heat capacity of the soil at 0% humidity can be seen below in Figure 5.

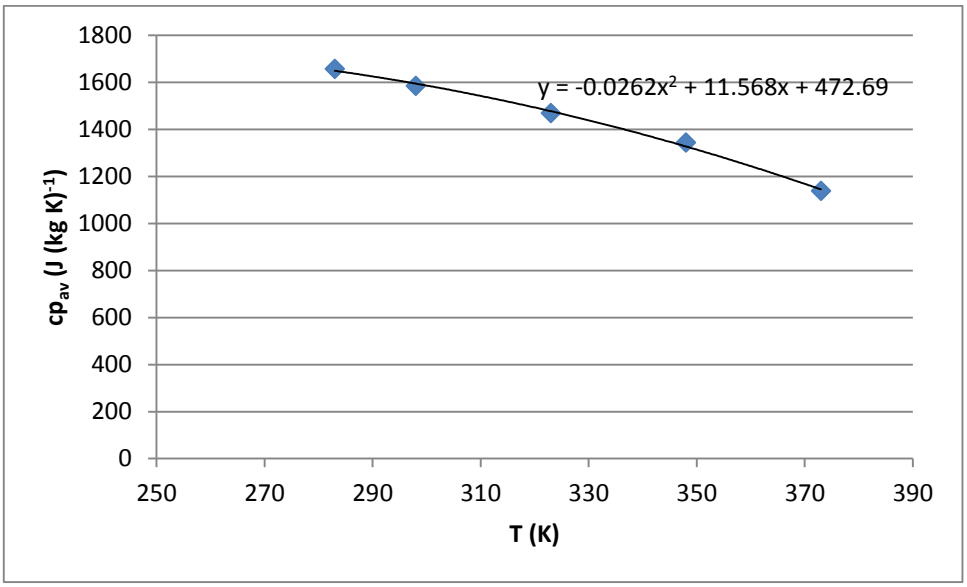

Figure 5: Variation in Specific Heat Capacity (c_p) in the soil model

Figure 5 indicates that the average specific heat capacity of the soil model can be seen to decrease over time. The rate of change of specific heat capacity increases in conjunction with the increase in phase change across the temperature range from the vapour phase to the liquid phase. The maximum heat capacity of this soil model occurs where there has been zero phase change, at the starting temperature of 283 K before heat has been applied to the soil 1657 J (kg K)$^{-1}$, whilst the minimum value occurs when all the water has transferred from the liquid phase to the vapour phase with a value of 1139 J (kg K)$^{-1}$. At this minimum value the

rate of temperature change within the soil is significantly higher than the rate at the maximum. This indicates that as phase change continues throughout the soil model, the models ability to store heat will diminish over time as its average specific heat capacity decreases.

3.3 Change in Soil composition with time

Having calculated the relative time taken to bring about the temperature change within the soil, and having calculated the potential evaporation rate within the soil, Figure 6 (shown below) shows how the composition of the soil varies with time.

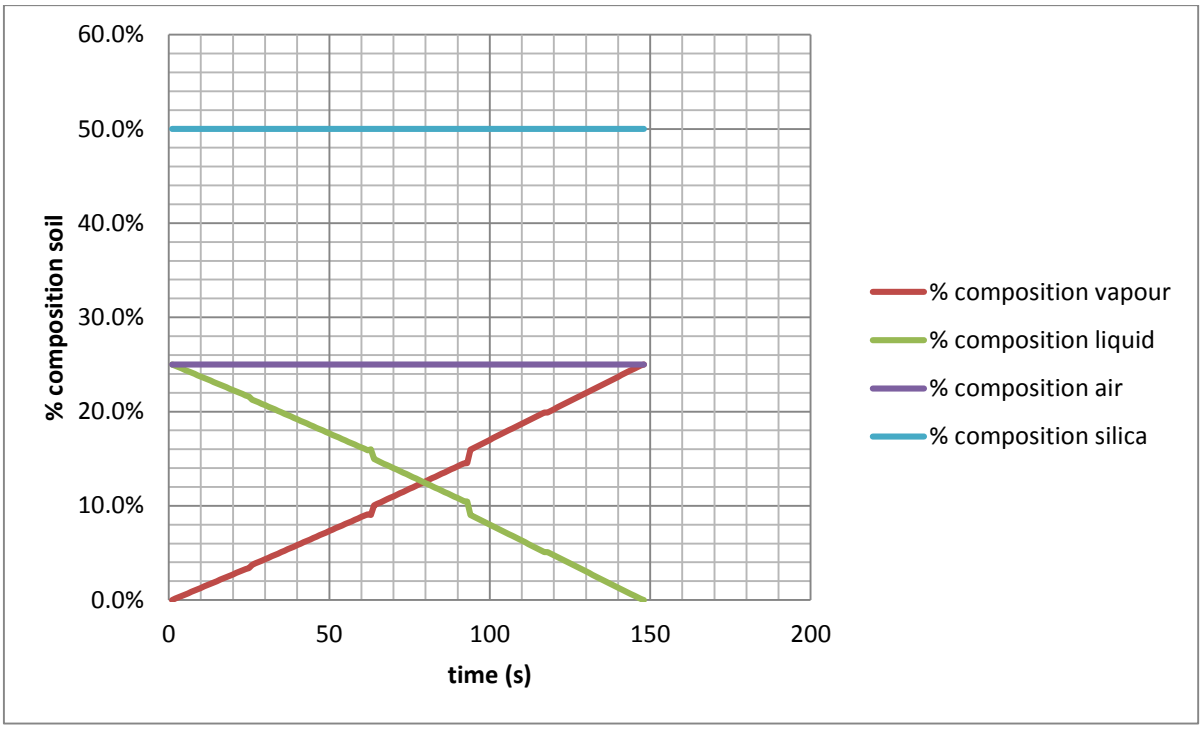

Figure 6: The phase change in the soil at 0% humidity

From Figure 6, the phase change with time appears to be relatively constant as time goes on. On the liquid and vapour lines of the chart, slight fluctuations can be observed at 23, 61, and 96 seconds. These fluctuations represent the variation in evaporation rate as the overall temperature of the soil increases. Since the evaporation rate at 283 K and 298 K are so similar (0.057 and 0.06 kg s-1, respectively) the variation in gradient of the % phase change line for both vapour and liquid is indiscernible, but as the rate of evaporation within the model increases to 0.064 and 0.069 kg s-1 at 323 and 348 K, the increasing rate of phase change can be observed. From the above chart, it can be seen that for complete phase change to occur based on the evaporation rate calculated, the total time is approximately 150 s. At an initial soil temperature of 373 K, it is assumed that the mass fraction of the liquid phase within the

soil is equal to 0, ie that complete phase change has occured. Therefore Figure 6 indicates the total time allowing for complete phase change to occur within the soil based on the composition of the soil at 348 K.

From this study into the variation of heat capacity within the soil model, the thermal analysis has shown that the heat capacity of the soil tends towards its minimum as the rate of change in temperature within the soil model increases to its maximum, along with the evaporation rate calculated for the model.

This study into the variation in heat capacity with temperature is important to the understanding of the subsurface of the earth to be used as a potential heat reservoir. The amount of heat applied to the soil has a direct effect on the soil temperature and as the temperature within the soil increases, the phase change with evaporation rate increases. This causes an increase in the rate of temperature change within the soil. As a result, a significant drop off in the average specific heat capacity of the model can be seen, and the models potential to be used as an effective thermo-geology heat source reduces significantly.

3.4 Internal Energy of the soil

Appendix C shows the data used for the investigation into the variation in internal energy of the soil.

The previous investigation into the rate of phase change within the soil allowed the variation in soil composition to be calculated. The table shown below indicates the phase change at the given temperatures, allowing the internal energy of each phase to be calculated.

T (K)	x quartz	x air	x liquid	x vapour
283	0.5	0.25	0.25	0
298	0.5	0.25	0.22	0.03
323	0.5	0.25	0.16	0.09
348	0.5	0.25	0.10	0.15
373	0.5	0.25	0	0.25

Table 4: Phase composition at 0% humidity

The change in internal energy was then calculated based the composition of the soil shown above, by summation of the internal energy of each phase. Below, in Figure 7, the percentage composition of the change in internal energy of the overall soil model can be seen. To calculate the actual change in internal energy of the phases within the soil model,

the latent heat, previously ignored, was calculated as a function of the mass of the water vapour at the final temperature. Furthermore, since the volume of water vapour per mass is significantly more than the volume of liquid volume of equal mass, it suggests that significant work must be done upon the liquid when it changes phase into a vapour, which must be calculated and taken away from the total internal energy calculated.

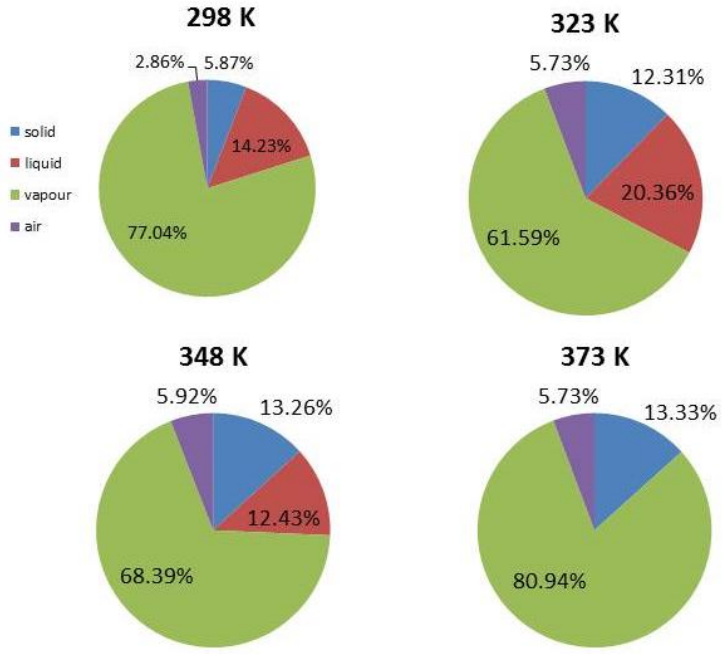

Figure 7: Variation in dU with temperature at 0% humidity

At 298 K a significant slice of the total change in internal energy within the soil comes liquid phase (14.2%), with the solid phase containing 5.87 % and the gaseous phase with 2.86 %. It is important to note that though the mass fraction of vapour at 298 K is just 0.03, the latent heat required by the liquid phase to enter the vapour phase results in it accounting for 77% of the total internal energy change at ΔT = 15 K. The liquid phase undergoes a strange transition throughout this study, initially beginning at 14.23 % at 298, before increasing to 20.36 % at 323 K, even as its phase change reduces. This gives an indication of the effect of waters large specific heat capacity, though as the phase change continues at 348 K, the liquid phase accounts for just 12.43 %, before completely disappearing in the vapour phase. The solid phase increases across the temperature range, starting at 5.9 % before increasing to ≈13 % at 373 K. The gaseous phase changes very slightly as a function of temperature. Since it is a function of only the temperature, it remains between 5 – 6 % of the total change in

internal energy across the temperature range. This trend is repeated in Figure 8, where the linear increase in the internal energy of the phases can be seen.

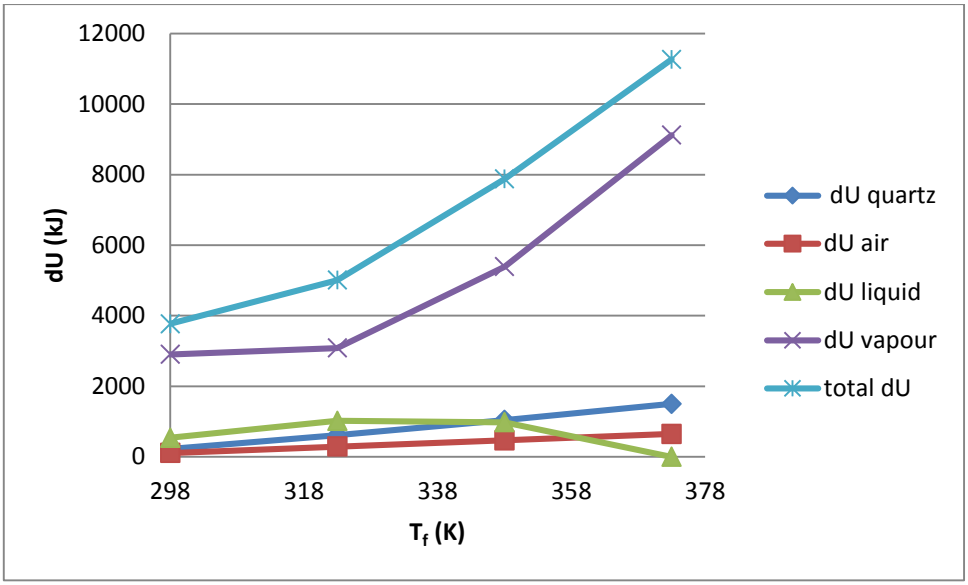

Figure 8: Change in Internal Energy contribution per phase

Initially, the *d*U of the vapour phase appears to remain relatively constant from 298K to 323 K, however this is due to the much greater work done at 323 K, reducing the impact on *d*U. As the phase change within the model increases, and the latent heat increases significantly, the calculated work done is overcome. This underlines the impact of the amount of latent heat absorbed to move into the vapour phase. Across the temperature range, the change in internal energy increases from 3768 kJ at 298 K, up to around 11,000 kJ at 373 K. This represents a 5 fold increase over the temperature range. In contrast, the liquid phase initially shows an upward trend as the change in temperature of the model effects the internal energy, before the phase change in the model results in a decreasing effect of the liquid phase on the total internal energy phase in the model. Both the solid phase and the gaseous phase within the soil increase steadily as a function of the temperature, but as shown in Figure 8 the overall effect on internal energy palls in comparison to the effect of the vapour phase.

The significant latent heat absorbed by the liquid phase as it transitions into the vapour phase results in a steep increase in its internal energy. Assuming no energy is lost to the surroundings, when the soil cools, this latent heat from the vapour phase would be released back into the soil system resulting in an increase in the temperature of the localized atmosphere within the soil. In a heat storage system, this could be used to boost the overall

efficiency of a heat pump system, although gases are very poor insulators of heat, and this rapid cooling would likely result in the energy being lost rapidly, as it is unlikely the heat transfer fluid used would be able to readily collect the sudden latent heat released.

3.5 Change in Entropy of the Soil Model

The entropy change within the soil model can be used to determine the "level of disorder" within the system. The full sets of data required for the study into entropy change are listed in Appendix D. Figure 9 shows how the change in entropy of the system can split into the individual phases of the model.

From Figure 9, it can be seen that across the temperature range the majority of the entropy change taking place comes from the vapour phase, which shows a steady upwards trend from 77% up to 91% as the liquid phase disappears. As the mass fraction of the vapour phase increases, the contribution to the total entropy change from the liquid phase decreases across the temperature range from 13.5 % to 298 K to ≈10 % at 323 K, and then 6% at 348 K before disappearing completely at 373 K. An explanation for this is that even though at 298 K the mass fraction of the vapour phase is minimal, the entropy increase as a result of the phase change is significant (dS_{vap} = 40.65 kJ/mol). The significant ΔS increase for the vapour phase comes in conjunction to the decreasing percentage change shown in the liquid phase, as its mass fraction within the soil model reduces. In contrast, both the solid and air phases within the soil model remain relatively consistent (quartz 5 – 6 %, air ≈ 3.7 %) across the temperature range, where the change in entropy depends solely on the heat added to the system, along with the change in temperature.

Figure 9: Variation in ΔS with soil temperature

The overall trend in total entropy change within the system can be seen in Figure 10 where an almost linear relationship between the vapour phase and total entropy change which highlights the size of the contribution from the vapour phase, as previously indicated by the investigation into the change in internal energy of the soil model. The solid and air phases within the soil show a linear increase across the temperature range, while as anticipated the liquid phase begins higher than the solid and air phase due in part to the large specific heat value of water (c_p, in this case), though this begins to decrease as the phase change occurs within the soil.

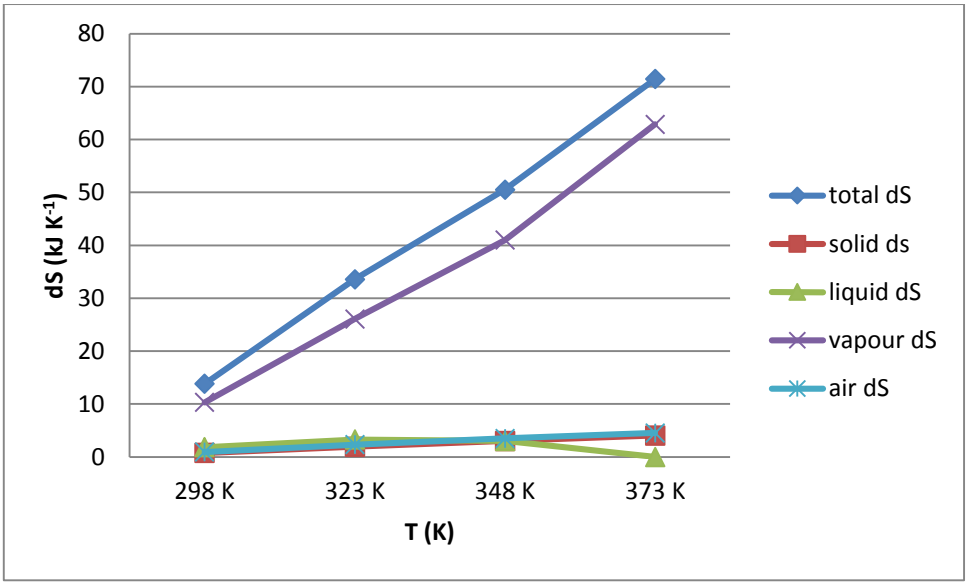

Figure 10: Variation in dS per phase

Assuming the process remains at thermodynamic equilibrium throughout the heating process, the heat added to the system can be viewed as a reversible. With this in mind, the total entropy change of the system and the surrounding universe must be equal to zero. Within this study into the effects of heating the soil model, and its impact on entropy within the system, the disproportionate relationship between the entropy of the vapour phase and the other phases in the soil indicate the significant disorder within the vapour phase. Furthermore, since this model is based on a closed system not exchanging heat with its surroundings at thermal equilibrium, it suggests that there will be conservation of heat, this massive increase in entropy change which has been calculated, would require an equal and opposite change in entropy where the excess heat were being removed from the atmosphere and transferred to the soil, through the heat pump system. The effect of removing that much heat from a building through an exhaust vent (or the return of hot heat transfer fluid to the soil), would result in the formation of mist as any water vapour in the atmosphere where the heat is removed would have to lose a significant amount of latent heat to allow the $\Delta S = 0$ within the system.

3.6 Study into the effects of heat removal within the soil

3.6.1 Change in Entropy as heat is removed from soil

The thermal analysis of a novel space heating system using the ground as a medium of heat storage requires an analysis of the impact of heat removal from the soil. Assuming that the soil is at the initial temperature of 283 K, and heat is then removed down to a temperature of 263 K, an analysis into the effect of this change in temperature on *dS* and *dU* within the soil model was investigated. At 273 K, it was assumed that enough heat had been removed from the soil to result in the anticipated temperature change, but not enough heat to cause phase change within the liquid phase of the soil. The full sets of data required for the study into the removal of heat from the homogeneous soil model are listed in Appendix E. In Figure 11, the impact on the formation of ice on the total entropy change within the system can be seen. Since entropy is a measure of the level of disorder within a system, the negative entropy indicated in this analysis indicates that there is a significant increase in the order within the system. As the liquid phase freezes into the solid phase, its entropy decreases as a function of the number of moles within the system and ΔS_{fus} for water. The effect is similar to that of the increase in entropy in the vapour phase when heat is added to the system, the total entropy of the system appears almost as a linear function of the phase. Figure 11 below shows the change in entropy of the soil between 283 K reducing to 273, and 263 K respectively.

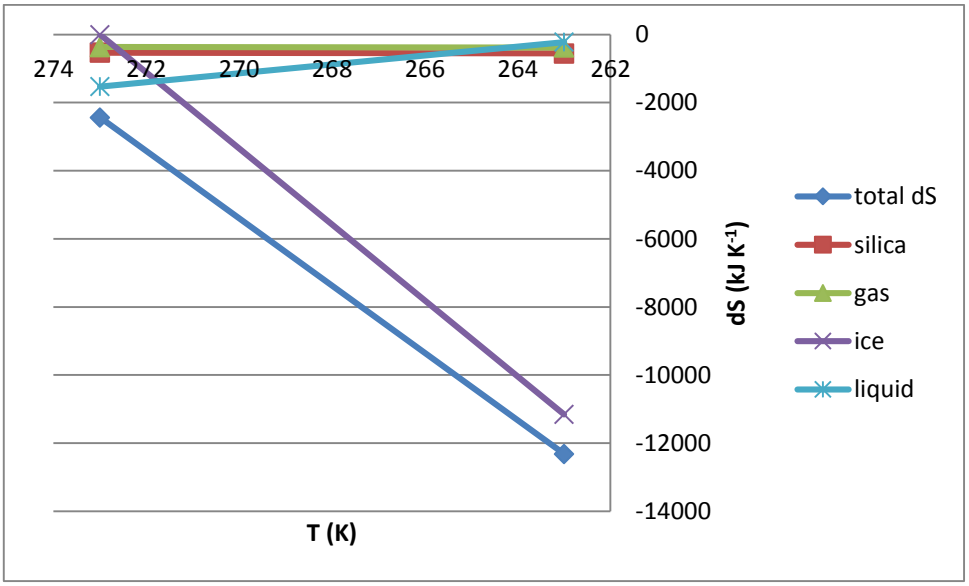

Figure 11: Variation in Entropy change as heat is removed from system

From 283 – 273 K, the total heat removed from the soil model was calculated as 664.6 kJ of energy, indicating the available energy available within the soil for a GSHP cycle. From 273 – 263 K, the heat removed is equal to 479.85 kJ, which indicates the impact of the reduction of specific heat capacity as the water within the soil model freezes. The change in heat over the dT = 10 K ranges indicate liquid water's special ability to store heat. As the phase change occurs and the mass fraction of liquid reduces, the maximum heat storage potential within the soil model reduces also. The difference in energy stored is accentuated by the significant latent heat released by the liquid phase (2870 kJ) based on the 40 kg model.

From the pie charts shown in Figure 12, the impact of the freezing of ice on the entropy change is clear. At 273 K, before phase change occurs, the percentage *dS* of the liquid phase accounts for 62.9 %. This decreases to 3.1 % at 263 K (or 444 J, Figure 12), though the total entropy change from the water component (both liquid and vapour phases combined) in the soil increases to 87.2 %, with the majority (84.1 %, 122 kJ) coming from the change in entropy of the solid water phase. This significant decrease in entropy is caused by the latent heat released by the liquid phase, which results in the significant negative entropy change during the phase transition into solid ice. The linear decrease in entropy change between both the gaseous phase and the solid quartz phase within the system shows a steady relationship between total entropy change and the temperature of the system. From Figure 12 we can see that the contribution for the total entropy change of the system decreases from 22% to just 7.6 % in the solid phase, whilst the gaseous phase reduces from 15.1 % at 273 K to 5.3 % at 263 K. This highlights the significant increase in the order of the soil model as a result due to the solidification of water. Once again, treating the system as a reversible process dS = 0, the assumption from this study into the variation in entropy as the soil temperature decreases, is that there must be an equal increase in entropy change where the heat removed from the system is being utilized (ie. the building being heated up).

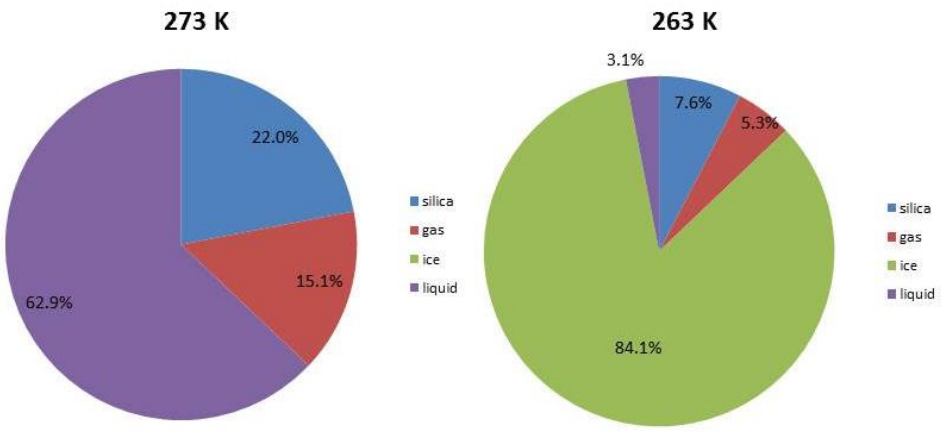

Figure 12: Variation in Entropy as heat is removed from system

In this study into the variation in entropy as the heat is removed from the soil, it can be concluded that the majority of the change in entropy within the soil model comes from the water component. For the liquid to move into the solid phase, a significant amount of latent heat is released from the soil model, which results in a large increase in entropy change, and is therefore available to a heating cycle. As mentioned in the previous study into internal energy, being able to remove this latent heat effectively will result in an energy "boost" within the heat pump configuration, whilst reducing the soil model to a more ordered structure, hence the significant decrease in entropy change. The difference in specific heat capacity between water and ice indicates, however, that on returning heat to the soil at an initial temperature of 263 K, the models ability to store the energy over a period of time while ice remains as a component is reduced, and is therefore unlikely to be the most efficient use of the subsurface as a heat sink.

3.6.2 The Variation in Internal Energy as heat is removed from the soil system

Following the completion into the variation of entropy within the soil when heat is removed, an investigation was carried out into the impact on the change in internal energy within the system as heat is removed from the system.

As previously mentioned in the study into the change in entropy as heat is removed from the soil model, and in contrast to the absorption of latent heat when the water component moves from the liquid phase into the vapour phase, when heat is removed from the system latent

heat is released by the liquid phase. As the entropy of the system decreases so too does the internal energy within the system. In Figure 13, the composition of the change in internal energy within each phase is shown.

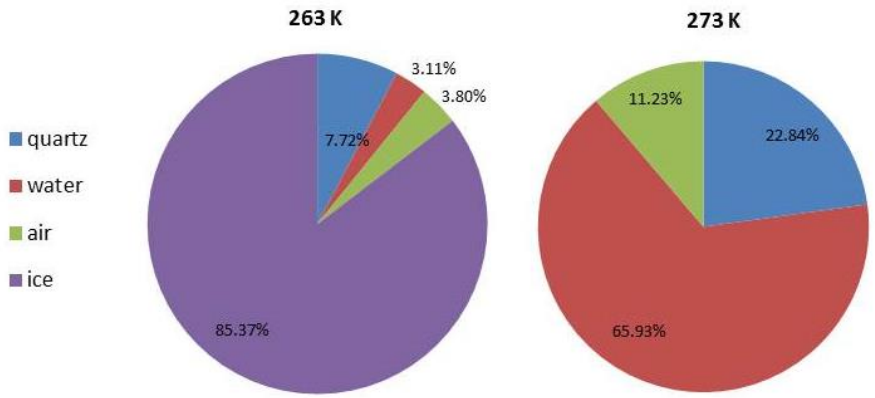

Figure 13: Variation in Internal Energy as heat is removed

In the transition between 273 K to 263 K, we can see that the water phase contribution of 66 % increases to around 85.37 % of the change in total internal energy of the soil model. This is due to the heat released by the liquid phase moving into the solid phase is removed from the internal energy of the solid phase, since the molecules making up the ice have significantly less ability to rotate within the ice lattice, resulting in a significant decrease in internal energy of the model. Had no phase change occurred, the change in internal energy of the water component would decrease linearly between the two temperatures. The significant decrease in internal energy of the soil model due to the solidification of water is highlighted by the reduction in percentage composition of *d*U from both the gaseous phase and the quartz phase which reduce from 11.23 % - 3.8 % and 22.84 % - 7.72 % respectively. The gaseous phase and the quartz phase both share a linear relationship with temperature, as shown in Figure 14, though the contribution from these phases is dwarfed by the contribution from the ice phase in the model.

Figure 14 below shows the change in internal energy within each phase in the soil model. The change in internal energy of the quartz is unsighted behind the *dU* of air which has a very similair change to it.

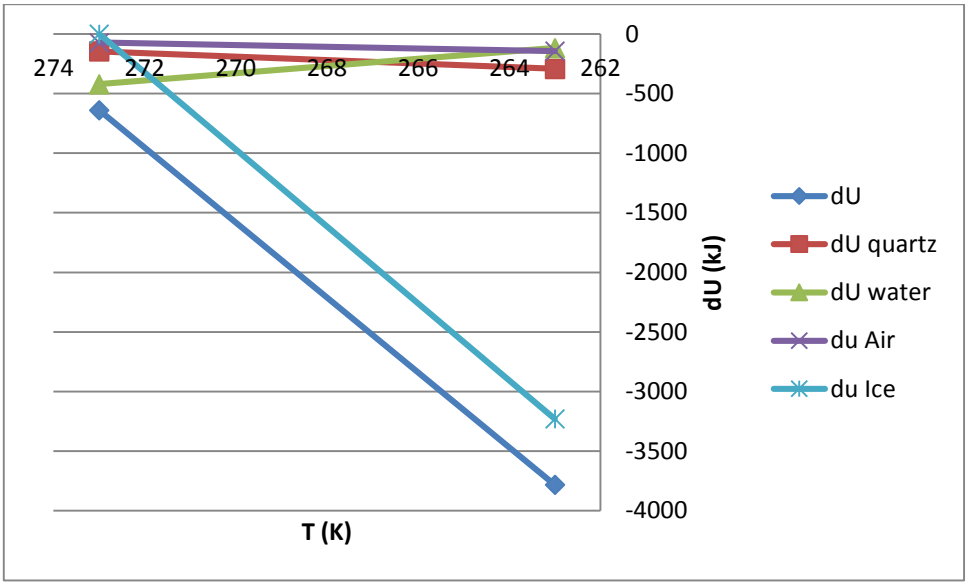

Figure 14: Overall variation in dU as heat is removed from soil model

From the chart, the decreasing contribution to the total internal energy of the water from 273 – 263 K is clear, as well as the corresponding increase in *dU* by the ice phase in the system. However, where the *dU* of the the liquid phase is -421 kJ at 273 K, at the minimum temperature following the phase change within the system, the *dU* for the ice phase is -3230 kJ, indicating the significant amount of latent heat released by the liquid phase as the phase transition to ice occurs (2877 kJ). As can be seen in this study, the internal energy of the soil model decreases significantly as heat is removed from the system. As the mass fraction of the vapour phase reduces to just 0.035, its large specific heat means it retains a significant amount of internal energy change, -117 kJ, which is comparable with the *d*U of the gaseous phase, of -143.6 kJ, though the gaseous phase has a fixed mass fraction of 0.25.

For this study into the thermal analysis of the soil as a heat storage medium in thermo-geology, understanding the energy breakdown of the phases is of particular importance. Since the heat capacity of ice is lower than that of water, the ability for the ice phase to increase its temperature within the soil is quicker than that of the liquid phase. However in a practical situation, where the heat being removed for the soil is used as part of a heat pump system, the removal of heat from the soil below the freezing point of water would result in a dumping of heat into the local environment within the soil, as the liquid phase solidifies. With the use

of a thorough ground-sourced heat pump system, with multiple loops of heat transfer fluid, this excess heat could be collected and returned to be used as part of the system. However, when adding heat back into the soil, the frozen ice within the soil would have to reabsorb the latent heat of fusion to move back into the liquid phase to increase the overall temperature within the soil, which is disadvantageous, since it is the liquid phase that stores the heat energy so effectively.

3.7 Study into the heat required by the soil as a function of humidity

As previously mentioned while calculating the initial evaporation rate, humidity will have an impact on the specific heat capacity both at constant pressure and at constant volume. In perspective, this would suggest that depending on humidity conditions within the soil, the specific heat capacity will fluctuate, and the *Q* required to raise the temperature of the soil will also vary. Figure 15 shows how the specific heat capacity of the soil mixture varies with the humidity. Appendix F indicates the data required to calculate the variation in specific heat capacity of the soil as a function of the humidity.

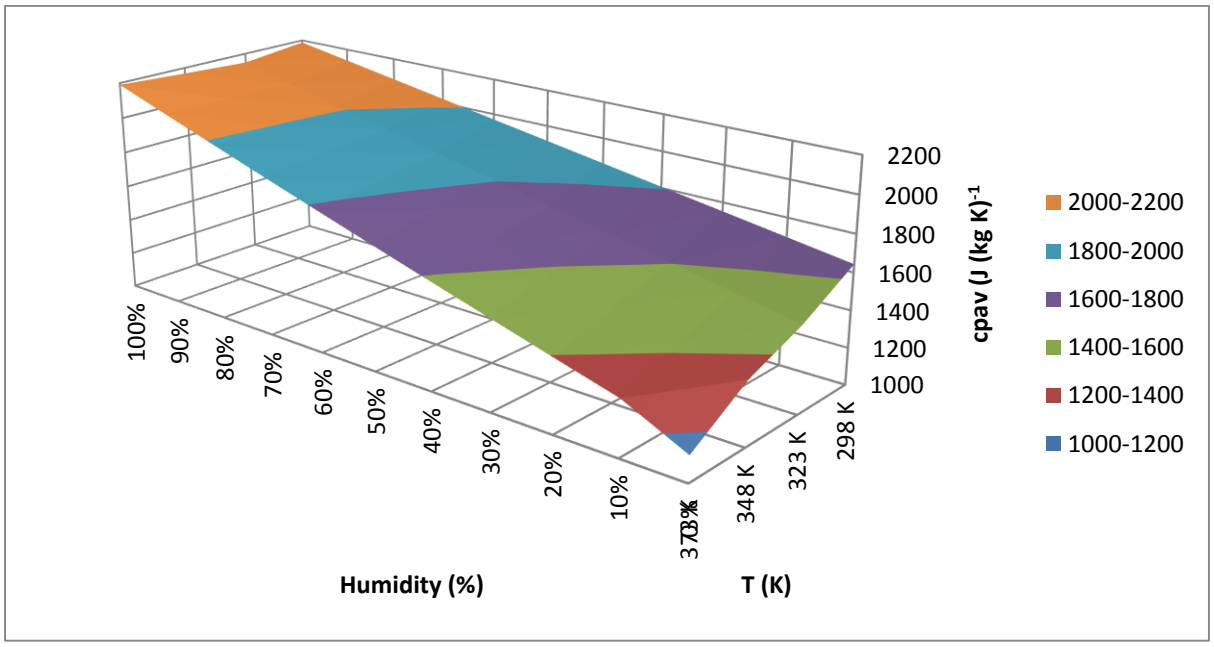

Figure 15: Variation in cp with humidity

Figure 15 shows the direct effect on the variation in specific heat capacity with the soil due to the humidity conditions. There is an upwards trend across the temperature range for the specific heat capacity of the soil as humidity increases. This is due to the increased vapour component within the air, resulting in a steady increase in the specific heat capacity of the air as humidity increases, since the mass fraction of the gaseous phase remains constant throughout this study. The variation in heat capacity of the gaseous phase is shown in Appendix F.1. As a result of the increase in humidity, the greatest variation in specific heat capacity occurs at the highest temperature of this study (373 K) where at 0% humidity the average specific heat capacity of the soil is equal to 1138 J/ kg K, increasing up to 2190 J/ (kg K)$^{-1}$. This is due to the reducing phase change as the humidity within the soil results in a decrease in the vapour pressure deficit, which causes a drop in evaporation rate in the model. As a result, the liquid phase in the soil model retains an increased mass fraction compared to the vapour phase, where the overall effect is an increase in average specific heat capacity, on top of the increase calculated due to the humidity of the gaseous phase. This trend continues across the full temperature range, from 298 K – 373 K, resulting in a steady increase in the average specific heat capacity of the soil as humidity increases. At 100% humidity, where no phase change will occur, Figure 15 shows a plateau across the chart, with the only variations due to the slight fluctuations in specific heats of the components as a function of the model temperature.

Having identified the impact of humidity upon the average specific heat capacity of the soil, the following investigation into the variation in heat required by the soil to increase the temperature was carried out. Figure 16 indicates the results of the study into the variation in heat required by the soil as a function of increasing humidity within the soil model.

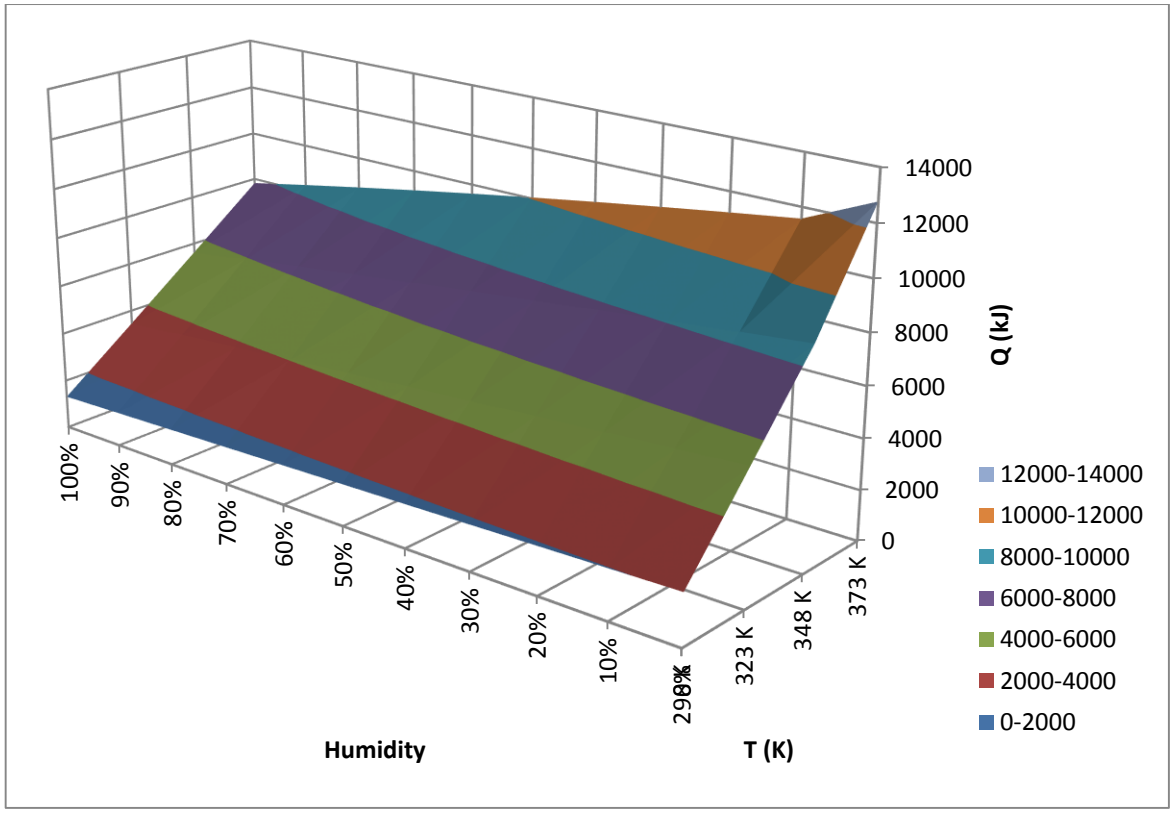

Figure 16: Variation in heat required with humidity

Figure 16 indicates a decreasing trend in heat required to increase the temperature of the soil model from the initial (283 K) as humidity increases. The highest value for heat required by the soil occurs across the temperature range occurs at 0% humidity. The peak of the chart occurs therefore, at 0% humidity and with a final temperature of 373 K. This is due to the significant amount of latent heat that is absorbed by waters liquid phase to transition to the vapour phase (22,560 kJ), while at 100 % humidity, where phase change cannot occur just 2190.5 kJ of energy is required to increase the temperature from 348 K to 373 K. Across the temperature range this value remains relatively constant at 100% humidity, fluctuating between 2146.8 kJ between 298 and 323 K, to 2167.5 kJ between 323 – 348 K. While for the initial temperature change from 283 – 298 K, dT = 15 K, the heat required by the soil model is 1312 kJ. However, since this chart shows the summation of the heat required across the temperature range from 283 – 373 K, there is a steep upwards trend in the heat required at 100 % humidity, across the temperature range. On comparing the variation in heat required across the temperature range as humidity increases, the reduced phase change to Tf = 298 K means the downwards gradient of the heat required is significantly less than that at 373 K, where maximum phase change can occur at 0% humidity, but it is assumed no phase change

can be carried out at 373 K. Assuming any heat added to be reversible - aside from the work done on the system - as the mass fraction of the vapour phase reduces, the disorder within the system will decrease, which is shown below, Figure 17, in the investigation into the effect of humidity on the entropy change within the soil model.

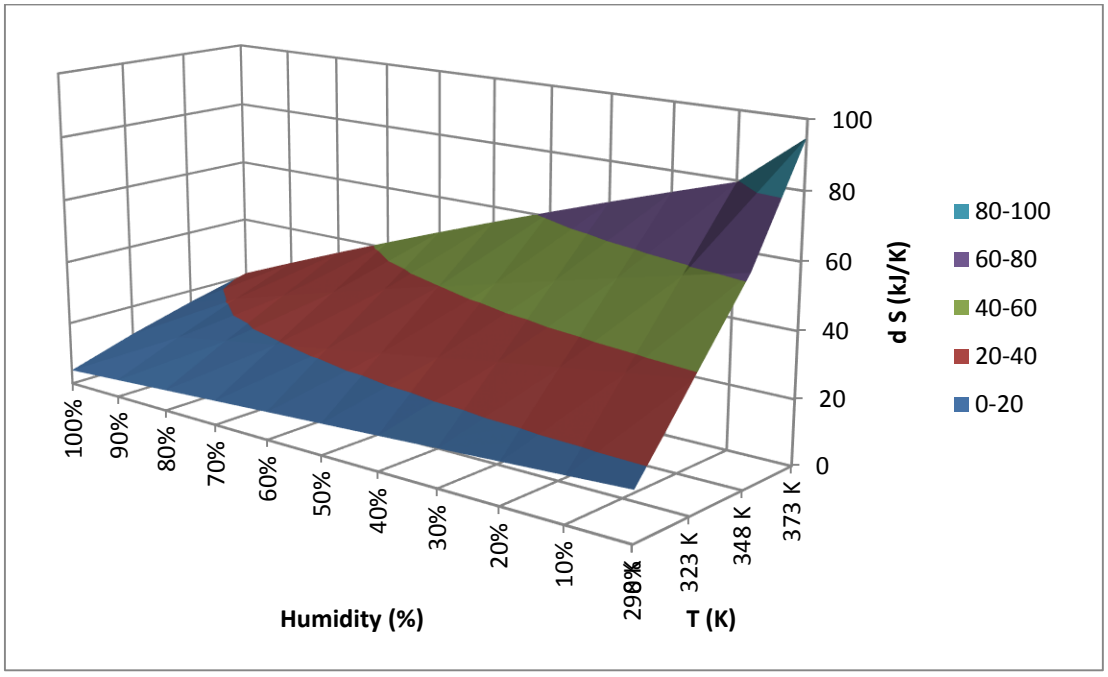

Figure 17: Variation in Entropy with humidity in the soil model

The data used to calculate the variation in entropy change with humidity is shown in Appendix F.2. From the figure it is clear that as the humidity increases, and the mass fraction of the vapour phase reduces with evaporation rate, the entropy change of the system also decreases. Since entropy is simply a function of the absolute temperature of the soil model, it follows exactly the same pattern as shown in the investigation into the heat required by the soil. At 100% humidity, since the absolute temperature of the soil model increases across the chart, the steady increase in entropy can be seen. From 0% humidity to 100% the change in entropy between each temperature steadily reduces from approximately 50 kJ/K at 0% humidity, to around 15 kJ/K at 100% humidity. As predicted this indicates that due to the reduction in phase change within the model, the resulting entropy change across the temperature range reduces significantly. This also means that the entropy of vaporization and its effect reduces

significantly as humidity increases, resulting in a much more thermodynamically efficient cycle.

This study into the variation in heat required due to increasing humidity conditions indicates that at a high level of humidity, the specific heat capacity will reach a peak due to the lack of phase change within the soil model. The result of this peak is twofold; the first point is that the heat required by the soil to increase the temperature overall will decrease, which is counter intuitive to what we would expect. This makes sense though, when looking at the latent heat of vaporization required by the liquid phase to move to the vapour phase. The second point, therefore, is that with increasing humidity and a decrease in phase change within the model, the overall heat required by the soil to change temperatures actually decreases, in conjunction to this, there is a significant decrease in the work done on the system, since the volumetric change from the liquid to the vapour phase can be ignored. In a practical application this indicates that by designing a heat pump system where the humidity of the soil could be varied either with human intervention or by a computer, the energy efficiency of the soil as a heat reservoir could be increased significantly.

3.8 Investigation into the effect of humidity on the Internal Energy of the soil model

Continuing the study into the impact of humidity on the specific heat capacity of the soil, the following study investigates the impact upon the specific heat capacity at constant volume for the soil. This will have a direct effect upon the internal energy of the soil. Appendix F indicates the data required to calculate the variation in cv of the soil, while Appendix F.3 indicates the variation in internal energy of the soil model.

Figure 18 shows the relationship between c_v and humidity as the composition of the soil varies with temperature.

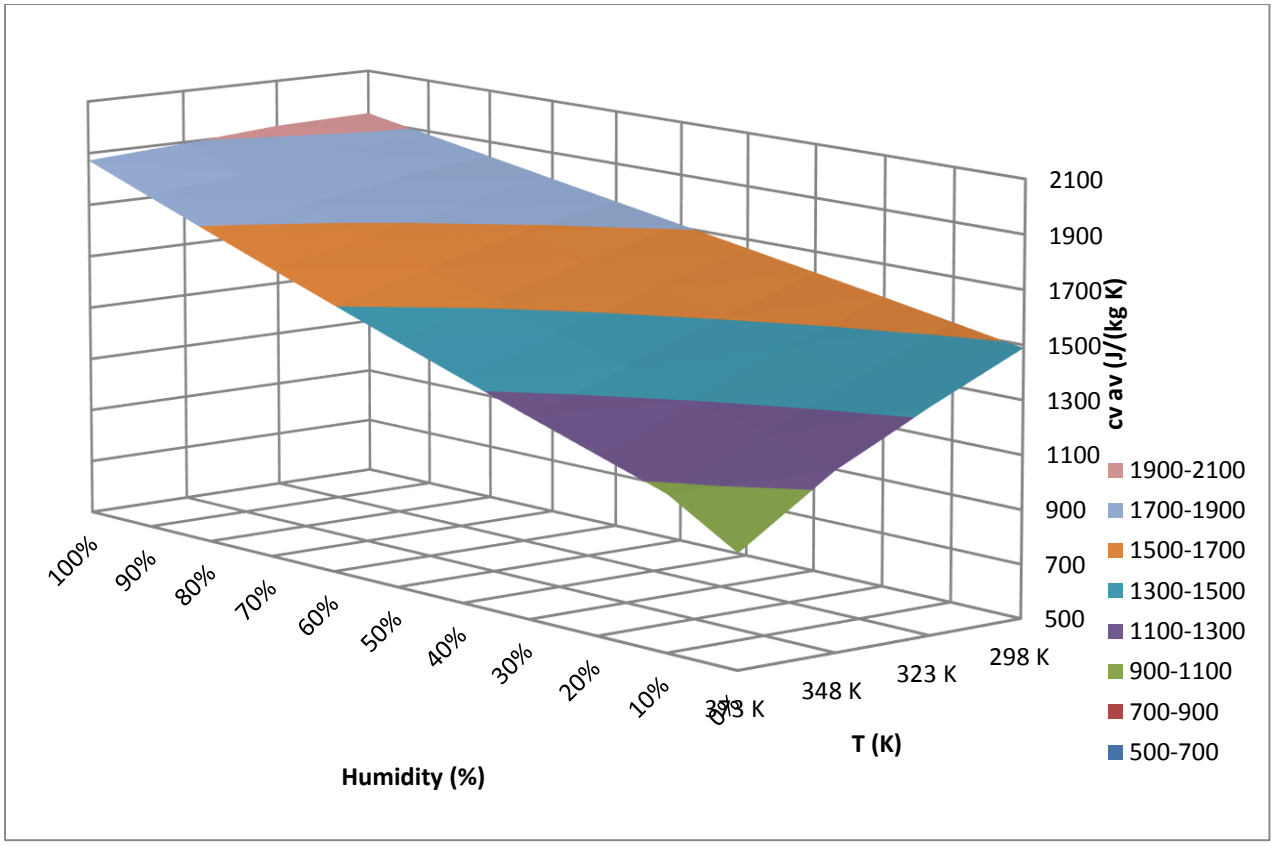

Figure 18: Variation in c_v with humidity in the soil model

As the specific heat capacity of the gaseous phase in this study increases with humidity, the overall trend in increasing c_v is anticipated. In the previous study into the variation in heat capacity the likewise trend was noted. As the humidity of the model increases and phase

change within the model decreases, the mass fraction of the liquid phase increases, resulting in itself an increase in the specific heat capacity. This, along with the increase in specific heat capacity of the gaseous phase, accounts for the general upwards trend in $c_v$av by the soil model across the temperature range. The minimal point in the plot occurs where the greatest mass fraction of vapour is present (373 K) and the humidity is at a minimum. This means that the cumulative effect of the substantial heat capacity of water as well as the increasing heat capacity of air with humidity cannot occur, and waters vapour phase has a significantly lower specific heat capacity than its liquid phase. At maximum humidity, there is a slight decrease in the specific heat capacity as temperature increases. This is due to the decreasing specific heat capacity of water at constant volume resulting in a very slight decrease overall average specific heat capacity of the model at constant volume.

The most important aspect of this study is the resulting increase in internal energy within the soil due to the increase in c_v. Figure 19 below shows the effect of humidity upon the internal energy of the soil model.

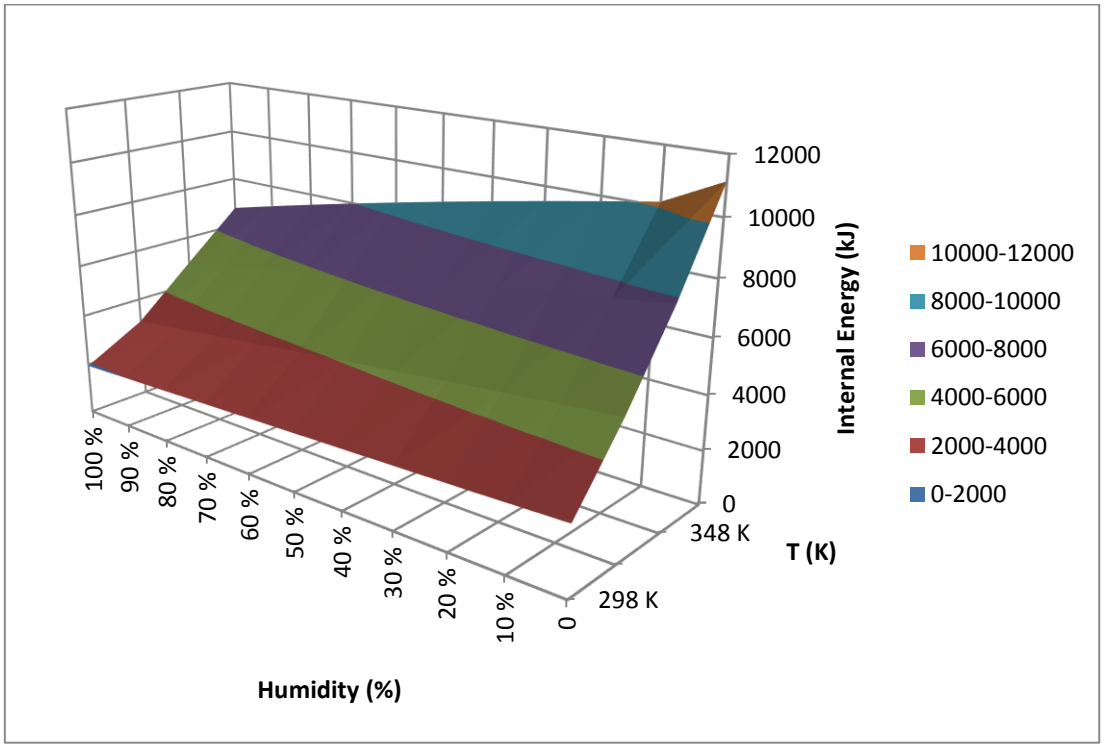

Figure 19: Variation in Internal Energy with humidity

From Figure 19, as humidity increases, the specific heat capacity for the gaseous phase increases steadily due to the increased component from liquid water and the increase in c_v for air. It could be assumed that this would result in an increase in the internal energy within the model, however as noted in the study into the effect of humidity on the heat required by the soil model, the opposite is true. The reduction in the amount of latent heat absorbed for the vaporization of the liquid phase means that it has significantly less kinetic energy than its vapour phase, although they are at the same temperature. This results in the general downwards trend in internal energy change within the homogeneous soil model, as the humidity within the model increases. At 100% humidity, the significant change in the internal energy across the temperature range is simply due to the increased dT of the model, resulting in a steep incline from 298 K to 373 K. This same trend can be seen across the whole humidity range, as the phase change within the model becomes a function purely of the humidity.

Fundamentally one of the most important conclusions of this study is the heat required for phase change within the soil is substantial due to the significant latent heat of vaporization for water. Specifically, if the soil was required to reach a temperature greater than 373 K, as shown in this study, there would a significant excess of heat required to be input to the system. In contrast to this, the specific heat capacity of liquid water is significantly higher than that of its vapour, indicating that it requires a greater energy input for each temperature change than its vapour, though this also shows waters ability to store heat is significantly greater than that of its vapour or its solid phase. However, this soil model is based upon the dynamic phase change within the earths subsurface as heat is applied. The transition from the liquid phase requires energy from the heat pump to be used to force this phase change, which ultimately is thermodynamically inefficient. In reality, the effect of this input of energy could result in a significant decrease in the coefficient of performance for the heat pump system, reducing the overall effectiveness of renewable heat from a thermo-geology source. In reflection, the most thermodynamically efficient system that could be designed to incorporate the use of the earths subsurface in a heat pump cycle would be that in which phase change could be minimized. Furthermore, it is far easier to design a system in which the phase change could be minimized since a waterproof reservoir could be designed relatively easily into which the soil could be added. This would allow the significant energy stored within the liquid phase to

remain there over a period of time, whilst in contrast, designing a system where the vapour phase was retained would be a far trickier proposal.

In this investigation into the variation in c_v of the soil, the impact of humidity can be seen to increase c_v at all temperatures. In a thermodynamically open system this increasing internal energy of the soil would be lost rapidly to the surrounding atmosphere. However, as previously mentioned, the significant increase in internal energy as a result of the increasing mass fraction of the vapour phase comes along with an increase in work done within the system, reducing the overall efficiency.

4 Conclusions

This project was undertaken to complete a thermal analysis of the earths subsurface as a potential heat reservoir to be utilized as part of a heat pump cycle. Initially the vapour pressure within the soil was investigated, and was used to calculate the potential evaporation rate within the soil. At 0% humidity the maximum evaporation rate was found to occur, and as the vapour pressure deficit within the soil decreased with increasing humidity, the rate of phase change within the soil was found to decrease to 0 kg s^{-1} at 100% humidity.

The preliminary study into phase change at 0% humidity showed that as evaporation rate increased with temperature, the maximum phase change within the soil could be found, and subsequently the variation in specific heat capacity was calculated. The conclusions of this initial study are that as temperature increased, the average specific heat capacity of the soil decreased to a minimum at 0% humidity and at a temperature of 373 K, where the remaining liquid phase of water evaporated into the vapour phase. The difference in specific heat capacity of water, being significantly higher than that of the vapour phase was proposed as the main reason for this decreasing trend across the temperature range.

This study investigated the change in internal energy as temperature of the homogeneous soil model increased. From the results it was clear that as the phase change within the model increased with temperature at 0% humidity, the change in internal energy increased almost linearly due to the significant internal energy of the vapour phase. This was concluded to be as a result of the significant heat of vaporization absorbed by the liquid phase as it transitioned into the vapour phase, resulting in a significant contribution in total internal energy change within the soil model.

The entropy change of the soil at different temperatures was investigated at 0% humidity, showing that as the temperature within the soil increased, the change in entropy within the soil increased. The liquid phase, before significant evaporation showed a significant contribution to the percentage dS within the soil model. As the phase change within the model increases, the entropy of vaporization results in the vapour phase contributing significantly to the change in entropy within the soil model. As this investigation was expanded to include increasing humidity within the soil, the evaporation rate decreased,

resulting in a significant reduction in the vapour phase mass fraction in comparison to 0% humidity.

Following the preliminary study into internal energy and entropy at 0% humidity, this was expanded to the full humidity range to determine its effect on dU and dS. As humidity increased, the study determined that the specific heat capacity (both c_p and c_v) increased steadily across the temperature range. The conclusions of this study indicated that the significant entropy of vaporization and heat of vaporization absorbed by the liquid phase reduced significantly as humidity increased. As a result of decreasing phase change as humidity increased, the energy required to increase the temperature of the soil decreased even as the specific heat capacity of the soil increased. This resulted in a significantly lower change in entropy across the temperature range as the level of disorder within the system decreased significantly. The study into internal energy of the soil model at varying temperature indicated that as phase change was minimized with humidity increasing, the internal energy of the system reduced, indicating that the most efficient design of a heat pump system using the earths subsurface as a heat reservoir would include a method to reduce phase change within the soil as temperature increases, perhaps by a method of humidity control.

5. Future considerations

Thermo-geology is a new science, and therefore there are lots of opportunities to expand this study across the globe.

- This project was based upon soil conditions commonly available within the UK, it would be relatively easy to expand this model to different initial conditions, particularly in parts of the world more willing to invest in renewable heat. Furthermore, an enhancement of the three phase model could be used, to investigate how the variation in molecular weight of the solid phase within the soil would have an impact on its ability to store heat.
- A practical study should be implemented to investigate the results within this study, if the conclusions remain accurate, the designs of a efficient GSHP cycle could be drawn up, particularly focussed on potential ways to control the humidity within the heat reservoir.
- It is important to expand the scope of this study to investigate the ability of the soil to store heat, and for what length of time. Increasing the efficiency of heat pump cycles is the clear purpose to thermo-geology, but the reality of returning heat back to the ground could prove futile if this heat diffuses further into the earths subsurface where it would be difficult to reuse.
- Finally, this preliminary study into a relatively new science was undertaken in an effort to increase the understanding of this science. With the global heat budget showing no signs of decreasing, studies into all forms of renewable heat will be fundamental to this generation. Investigations into the thermodynamics of the subsurface of the Earth must continue if a successful answer to the worlds problems are to be found.

6. References

[1] Energy Saving Trust, Ground Sourced Heat Pumps, Available from: http://www.energysavingtrust.org.uk/Generating-energy/Choosing-a-renewable-technology/Ground-source-heat-pumps [Accessed on 30th June 2014]

[2] D. Banks, Introduction to Thermogeology, Blackwell Publishing (2008) pg. 37.

[3] Temperature and Thermal Properties (Detailed), Natural Environment Research Council, Georeports, 4th May 2011.

[4] D. Banks, Introduction to Thermogeology, Blackwell Publishing (2008) pg. 68.

[5] I. N. Levine, Physical Chemistry, University of Brooklyn, Mcgraw-Hill Companies, 1978

[6]. D. Banks, Introduction to Thermogeology, Blackwell Publishing (2008) pg 69.

[7] "Arizona Master Gardener Manual". Cooperative Extension, College of Agriculture, University of Arizona. Chapter 2, pp 2–4. Available from : http://ag.arizona.edu/pubs/garden/mg/soils/soils.html [Accessed on 20th June 2014].

[8] K. Denbigh, The Principles of Chemical Equilibrium, Cambridge University Press, 1981, 4th Edition, pg 9.

[9] E.H Lieb, J. Yngvason, **The Physics and Mathematics of the second law of thermodynamics**, Physics Reports *1999*, p. 56.

[10] J. Newman, Physics of Life Sciences, Springer Science and Business media, (2008), pg 297.

[11] D. Banks, Introduction to Thermogeology, Blackwell Publishing (2008) pg 46

[12] K. Denbigh, The Principles of Chemical Equilibrium, Cambridge University Press, 1981, 4th Edition, pg 94.

[13] G. W. M. Thomson, **The Antoine Equation for Vapor-Pressure Data**, Chem. Rev., *1946*, pp 1–39.

[14] Dortmund Data bank, Available from : http://ddbonline.ddbst.com/AntoineCalculation/AntoineCalculationCGI.exe [accessed on 6th July 2014].

[15] Monteith, J. L., 1965. Evaporation and Environment. 19th Symposia of the Society for Experimental Biology, University Press, Cambridge, 19:205-234.

[16] E.K. Saxton., **Sensitivity analysis of the combination evapotranspiration equation**, Agricultural Meteorology, *1975,* 15, 343 -353.

[17] E.J. Sadler, D.E. Evans, Vapour pressure deficit calculations and their effect on the combination equation, **Agricultural and Forest Meteorology**, *1989*, 49, pp 55-80.

[18] Priestley, C.H.B., and R.J. Taylor, **On the assessment of surface heat flux and evaporation using large-scale parameters**. Mon. Weather Rev., *1972*,81-82.

[19] P. Kawamura, D. Mackay, (1987). **The evaporation of volatile liquids**, Journal of Hazardous Materials, *1987*, 343-364.

[20] K. Denbigh, The Principles of Chemical Equilibrium, Cambridge University Press, 1981, 4th Edition, pg 32.

[21] K. Denbigh, The Principles of Chemical Equilibrium, Cambridge University Press, 1981, 4th Edition, pg 42.

[22] K. Denbigh, The Principles of Chemical Equilibrium, Cambridge University Press, 1981, 4th Edition, pg 42.

[23] D. Eisenberg and W. Kauzmann, The structure and properties of water (Oxford University Press, London, 1969.

[24] K. Denbigh, The Principles of Chemical Equilibrium, Cambridge University Press, 1981, 4th Edition, pg 44.

[25] H. Fredriksson, U. Åkerlind , Physics of Functional Materials, Wiley, 2008, pg. 413.

[26] George Arfken, University Physics, Academic Press (1984) Ch. 22 thermal properties pg. 423.

[27] George Arfken, University Physics, Academic Press (1984) Ch. 22 thermal properties pg. 422.

[28] D. R. White, W. L.. Tew, ***Improved estimates of the isotopic correction constants for the triple point of water***, Int. J. Thermophysics, *2010* 31, pp. 1644-1653.

[29] Anderson. D.,, **The interface between ice and silicate surfaces**. Journal of colloid and interface sciences, *1967*, 171 – 191.

[30] D.R. Lide, Handbook of Chemistry and Physics, 73rd Edition, CRC Press, Boca Raton, 1992; Ch 6, pg. 10.

[31] R.B. Sosman, The Properties of Silica; an introduction to the properties of substances in the soilid-non conducting state, New York; The Chemical Catalogue company, *1927*, 37.

[32] M.R. Lindeburg Environmental Engineering reference manual for the PE exam, (2009), Professional publications, 51.7.

[33] M. Tooley, L. Dingle, BTEC National Engineering, Elselvier, Oxford, 2010.

[34] Engineering Toolbox; Available from: http://www.engineeringtoolbox.com/water-vapor-d_979.html. Accessed on 18th June 2014.

[35] National Physical Laboratory, Specific heat capacities. Available from : http://www.kayelaby.npl.co.uk/general_physics/2_3/2_3_6.html. Accessed on 18th June 2014.

7. Appendices

7.1 Appendix A

Below shows the data used to calculate the evaporation rate of the soil at a range of initial temperatures, based on the calculated vapour pressure deficit.

T (K)	Es (Pa)
283	14956.67
298	16440.49
323	19030.9
373	24594.08

Table 5: Variation in Saturation pressure with temperature

Humidity (%)	Ea (Pa)	VPD (Pa)	E (kg s^{-1}) 283 K
0	0	14957	0.0572
10	1496	13461	0.0515
20	2991	11965	0.0458
30	4487	10470	0.0400
40	5983	8974	0.0343
50	7478	7478	0.0286
60	8974	5983	0.0229
70	10470	4487	0.0172
80	11965	2991	0.0114
90	13461	1496	0.0057
100	14957	0	0.0000

Table 6: Evaporation Rate at 283 K

Relative Humidity (%)	Ea (Pa)	VPD (Pa) 298K	E (kg s^{-1}) 298 K
0	0	16440	0.0597
10	1644	14796	0.0537
20	3288	13152	0.0478
30	4932	11508	0.0418
40	6576	9864	0.0358
50	8220	8220	0.0299
60	9864	6576	0.0239

70	11508	4932	0.0179
80	13152	3288	0.0119
90	14796	1644	0.0060
100	16440	0	0.0000

Table 7: Evaporation Rate at 298 K

Relative Humidity (%)	Ea (Pa)	VPD (Pa) 323 K	E (kg s^{-1}) 323 K
0	0	19031	0.0638
10	1903	17128	0.0574
20	3806	15225	0.0510
30	5709	13322	0.0446
40	7612	11419	0.0383
50	9515	9515	0.0319
60	11419	7612	0.0255
70	13322	5709	0.0191
80	15225	3806	0.0128
90	17128	1903	0.0064
100	19031	0	0.0000

Table 8: Evaporation Rate at 323 K

Relative Humidity (%)		VPD (Pa) 348K	E (kg s^{-1}) 348 K
0	0	21754	0.0687
10	2175	19579	0.0618
20	4351	17403	0.0549
30	6526	15228	0.0481
40	8702	13052	0.0412
50	10877	10877	0.0343
60	13052	8702	0.0275
70	15228	6526	0.0206
80	17403	4351	0.0137
90	19579	2175	0.0069
100	21754	0	0.0000

Table 9: Evaporation Rate at 348 K

Relative Humidity (%)	Ea (Pa)	VPD (Pa) 373 K	E (kg s^{-1}) 373 K
0	0	24594	0.0824
10	2459	22135	0.0742
20	4919	19675	0.0659
30	7378	17216	0.0577
40	9838	14756	0.0495
50	12297	12297	0.0412
60	14756	9838	0.0330
70	17216	7378	0.0247
80	19675	4919	0.0165
90	22135	2459	0.0082
100	24594	0	0.0000

Table 10: Evaporation Rate at 373 K

7.2 Appendix B

The Investigation into the variation in heat capacities as a function of the temperature and phase change within the soil model.

Tables 10, 11 and 12 below indicate the calculated phase change within the soil at 0% humidity, and the variation in specific heat capacities calculated across the temperature range. The references for specific heats are given below. Water. [30] Quartz. [31] Air cp [32] cv [33]. Water Vapour cp [34] cv calculated from ratio of specific heats given in [35]. Any values not listed were calculated using interpolation. For water, the ratio of specific heat capacities was calculated using the following equation;

$$c_v = c_p - \frac{a^2}{\beta_T P}$$

Initial Temperature	x quartz	x air	x water	x vapour
283	0.5	0.25	0.25	0
298	0.5	0.25	0.219964	0.030036
323	0.5	0.25	0.158268	0.091732
348	0.5	0.25	0.095909	0.154091

Table 11: Phase Change at 0% humidity

T (K)	cp quartz	cp air	cp water	cp water vap	average cp
283	715.902	1005	4192.1	1857	1657.226
298	736.998	1005	4179.6	1859.8	1343.722
323	770.958	1005	4180.6	1865.32	1218.243
348	803.418	1005	4192.7	1872.104	1343.551

Table 12: Variation in c_p at 0% humidity

T (K)	C_v quartz J (kg K)$^{-1}$	C_v air	cv water	c_v water vap	average c_v
283	736.998	718	4136	1398.346	1320.271
298	770.958	718	4028.1	1402.496	1151.651
323	770.958	718	3912.9	1407.597	977.6587
348	770.958	718	3814.4	1413.632	956.7148

Table 13: Variation in c_v at 0% humidity

Heat required

The heat input to the soil required for the temperature change listed can be shown below. It was assumed that to calculate the phase change based on the evaporation rate within the soil, that the latent heat of vaporization was not absorbed during this study, though it is listed in Table 13 as it is required in subsequent calculations.

Initial Temp	Final Temp (K)	dT (K)	Rate of temperature change (K s-1)	Heat Required (kJ)	T (s)	Total Heat (kJ)	total time (s)	latent heat required (kJ)
283	298	15	0.634	994	23.67	994	23.67	3055
298	323	25	0.662	1586	37.76	2580	61.44	8278
323	348	25	0.715	1469	34.99	4050	96.43	13875
348	373	25	0.781	1344	32.01	5395	128.44	22560

Table 14: Investigation into heat required for temperature change at 0% humidity

7.3 Appendix C

When calculating the internal energy of the soil model it was assumed that there was no volume change in the gaseous phase from the air as it had such a small

Table 14 indicates the latent heat absorbed by the liquid phase as it transitions to the vapour phase, with the work done calculated based on a density of water across the

temperature range of 1000 g/m^3, these figures were used to calculate the change in internal energy per phase.

Tf (K)	Latent Heat (kJ)	Vapour volume (m^3)	equivalent liquid volume (m^3)	work done (kJ)
298	3055	1841	1.35	1840
323	8278	5406	3.67	5402
348	13875	9061	6.15	9055
373	22560	14733	10.0	14722

Table 15: Work done on the vapour phase

The composition of change in Internal Energy per phase

Tables 16 - 18 indicate the variation in internal energy at the given final temperature based on the phase composition calculated from the evaporation rate.

Material	cv J /kg K	mass fraction	mass (kg)	gfm (g)	n (kmoles)	delta U (kJ)	% composition
solid	736.998	0.5	20	60.08	0.333	221.0994	5.87%
liquid	4136	0.2161386	8.6455447	18	0.480	536.3695911	14.23%
vapour	1398.346	0.0338614	1.3544553	18	0.075	2903.276647	77.04%
air	718	0.25	10	28.97	0.345	107.7	2.86%
					total	3768.45	

Table 16: Phase contribution to Internal Energy change at 298 K

Material	cv J /kg K	mass fraction	mass (kg)	gfm (g)	n (kmoles)	delta U (kJ)	% composition
solid	770.958	0.5	20	60.08	0.3328895	616.7664	12.31%
liquid	4028.1	0.1582677	6.3307089	18	0.351706	1020.029137	20.36%
vapour	1402.496	0.0917323	3.6692911	18	0.2038495	3085.363626	61.59%
air	718	0.25	10	28.97	0.3451847	287.2	5.73%
					total	5009.359162	

Table 17: Phase contribution to Internal Energy change at 323 K

Material	cv J /kg K	mass fraction	mass (kg)	gfm (g)	n (kmoles)	delta U (kJ)	% composition
silica	803.42	0.5	20	60.08	0.333	1044.45	13.26%
liquid	3912.9	0.096	3.85	18	0.214	979.16	12.43%
vapour	1407.597	0.154	6.15	18	0.342	5389.12	68.39%
air	718	0.25	10	28.97	0.345	466.7	5.92%
					total	7879.42	

Table 18: Phase contribution to Internal Energy change at 348 K

Material	cv J /kg K	mass fraction	mass (kg)	gfm (g)	n (kmoles)	delta U (kJ)	% composition
silica	834.38	0.5	20	60.08	0.332889	1501.884	13.33%

liquid	3814.4	0	0	18	0	0	0.00%
vapour	1413.632	0.25	10	18	0.555556	9119.879532	80.94%
air	718	0.25	10	28.97	0.345185	646.2	5.73%
					total	11267.96353	

Table 19: Phase contribution to Internal Energy change at 373 K

The total Variation in Internal Energy, Figure 8, is shown below in Table 20.

Final T	dU quartz (kJ)	dU air (kJ)	dU liquid (kJ)	dU vapour (kJ)	total dU (kJ)
298	221.0994	107.7	536.3696	2903.277	3768.446
323	616.7664	287.2	1020.029	3085.364	5009.359
348	1044.446	466.7	979.1601	5389.116	7879.422
373	1501.884	646.2	0	9119.88	11267.96

Table 20: Variation in internal energy at 0% humidity

7.4 Appendix D

Investigation into the change in Entropy at 0% humidity

Table 21 below indicates the total entropy of vaporization based on the phase composition at the final temperature given. In this study, the entropy of vaporization = 108.951 J mol^{-1} K^{-1}.

Final T (K)	Entropy vap (kJ/ kmol)	n (kmols)	Total Entropy of vaporization (kJ)
298	108.951	0.075	10.25
323	108.951	0.204	25.63
348	108.951	0.342	39.87
373	108.951	0.556	60.48

Table 21: Entropy of Vaporization

The tables listed below (22- 25) indicate the data for the composition of dS from each phase in the soil model, including the addition of the entropy of vaporization in the total entropy calculate.

Material	cp	x	mass	Q	ds	composition
quartz	736.998	0.5	20	221.0994	0.74	0.055
liquid	4179.6	0.216	8.645545	542.0238	1.82	0.135
vapour	1859.8	0.034	1.354455	37.78524	10.39	0.772
air	1005	0.25	10	150.75	0.51	0.038

Table 22:Phase contribution to entropy change at 298 K

Material	cp	x	mass	Q	ds	composition
quartz	770.958	0.5	20	616.7664	1.91	0.058
liquid	4180.6	0.158	6.330709	1058.646	3.28	0.100
vapour	1865.32	0.092	3.669291	273.7761	26.50	0.805
air	1005	0.25	10	402	1.24	0.038

Table 23:Phase contribution to entropy change at 323 K

Material	cp	x	mass	Q	ds	composition
quartz	803.418	0.5	20	1044.443	3.00	0.060
liquid	4192.7	0.096	3.84983	1049.177	3.01	0.060
vapour	1872.1	0.154	6.15017	748.3926	42.06	0.842
air	1005	0.25	10	653.25	1.88	0.038

Table 24: Phase contribution to entropy change at 348 K

Material	cp	x	mass	Q	ds	composition
quartz	834.418	0.5	20	1501.952	4.03	0.056
liquid	4215.9	0	0	0	0.00	0.000
vapour	1880.13	0.25	10	1692.117	65.08	0.910
air	1005	0.25	10	904.5	2.42	0.034

Table 25: Phase contribution to entropy change at 373 K

Finally, the summary of the investigation into the variation in entropy with temperature at 0% humidity is listed below, Table 26.

Final T (K)	total dS (kJ/K)	solid ds (kJ/K)	liquid dS (kJ/K)	vapour dS (kJ/K)	air dS(kJ/K)
298	13.46	0.74	1.82	10.39	0.51
323	32.93	1.91	3.28	26.50	1.24
348	49.96	3.00	3.01	42.06	1.88
373	71.53	4.03	0	65.08	2.42

Table 26: Summary of results into entropy study

7.5 Appendix E

Investigation into the change in entropy and the change in internal energy as heat is removed from the soil model

Table 27 below shows the amount of heat required to be removed from the system, as well as the entropy change from 283 K to 273 K.

material	mass	gfm	n (kmols)	cp	dT	Q (kJ)	dS (kJ/K)	dS %
silica	20	60.08	0.3328895	730	-10	-146	-534.79853	0.219681
gas	10	28.97	0.3451847	1005	-10	-100.5	-368.13187	0.1512188
ice	0	18	0	2000	-10	0	0	0
liquid	10	18	0.5555556	4181	-10	-418.1	-1531.5018	0.6291002
					total	-664.6	-2434.4322	

Table 27: Variation in dS as heat removed from soil

At 263 K, it is assumed that 0.026g of water per gram quartz has remained unfrozen. The table 28 below indicates the total change in entropy (J/K) of the ice as a result of the heat released from the system.

ice (mass)	ice moles (kmols)	dS fusion	dS fusion	heat of fusion (kJ/mol)	Total heat released	heat removed	total dS
8.602791	0.477933	22	10514.5	6.02	2877.156	-169179	-11157.8

Table 28: Entropy change due to solidification of water

Table 29 below shows the composition of the change in entropy of the system.

Material	mass	gfm	n (kmols)	cp	dT	Total Q	dS	dS %
silica	20	60.08	0.3328895	730	-20	-292	-1110.3	0.08
gas	10	28.97	0.3451847	1005	-20	-201	-764.3	0.05
ice	8.6027907	18	0.4779328	2000	-20	-3217.44	-12233.6	0.84
liquid	1.3972093	18	0.0776227	4181	-20	-116.83	-444.2	0.03
						totoal	-14552.4	

Table 29: Total entropy change when heat is removed from system

Appendix E.2

Investigation into the change in entropy and the change in internal energy as heat is removed from the soil model

The table below shows the change in internal energy of the soil model, as heat is removed from the system. In table 30 the heat released was calculated as a function of delta H = 6.02 kJ/mol.

Composition at 273 K	mass	cv	gfm	n	dT	dU	% change dU
silica	20	730	60.08	0.332	-10	-146	22.84
water	10	4215.1	18	0.556	-10	-421.51	65.93
air	10	718	28.97	0.345	-10	-71.8	11.23
ice	0	2050.151	18	0	-10	0	0
					total	-639.31	

Table 30: Change in internal energy as Q removed from soil model. (273 K)

Final composition 263 K	mass	gfm	moles (kmols)	cv	dT	dU	heat released	actual dU	% change dU
silica	20	60.08	0.332889	730	-20	-292	0	-292	7.72
water	1.39709	18	0.077616	4215.1	-20	-117.777	0	-117.777	3.11
air	10	28.97	0.345185	718	-20	-143.6	0	-143.6	3.8
ice	8.60291	18	0.477939	2050.151	-20	-352.745	2877.195	-3229.94	85.37
					total	-906.123	Total	-3783.32	

Table 31: Change in internal energy as Q removed from soil (263 K)

Final T	dU	dU silica	dU water	du Air	du Ice
273	-639.31	-146	-421.51	-71.8	0
263	-3783.32	-292	-117.777	-143.6	-3229.94

Table 32: Change in internal energy across temperature range as heat is removed

7.6 Appendix F

The effect of humidity on phase change and subsequent heat required by the soil

Table 33 below shows the variation in the heat capacity of air with humidity, which can then be used to calculate the average specific heat capacity of the air.

Cpair (J (kg K)$^{-1}$)	0%	10%	20%	30%	40%	50%	60%	70%	80%	90%	100%
298 K	1005	1190.7	1376.4	1562.1	1747.8	1933.5	2119.2	2304.9	2490.6	2676.3	2862
323 k	1005	1190.98	1376.96	1562.94	1748.92	1934.9	2120.88	2306.86	2492.84	2678.8	2864.8
348 K	1005	1191.532	1378.06	1564.59	1751.13	1937.66	2124.19	2310.72	2497.26	2683.79	2870.3
373 K	1005	1192.21	1379.42	1566.63	1753.84	1941.05	2128.26	2315.47	2502.68	2689.89	2877.1

Table 33: Variation in Specific heat capacity (c_p) due to humdity

Tables 34 to 37 show the variation in phase change with humidity at each of the final temperatures based on the variation in evaporation rate calculated (Appendix A).

Humidity	x silica	x gas	x liquid	x vapour	heat capacity
0	0.5	0.25	0.2161	0.0339	1643.25
10	0.5	0.25	0.219525	0.030475	1697.68
20	0.5	0.25	0.222911	0.027089	1752.01
30	0.5	0.25	0.226297	0.023703	1806.34
40	0.5	0.25	0.229683	0.020317	1860.68

50	0.5	0.25	0.233069	0.016931	1915.013
60	0.5	0.25	0.236455	0.013545	1969.35
70	0.5	0.25	0.239842	0.010158	2023.68
80	0.5	0.25	0.243228	0.006772	2078.02
90	0.5	0.25	0.246614	0.003386	2132.35
100	0.5	0.25	0.25	0	2186.68

Table 34: Variation in phase change at t_f = 298 K

Humidity	x silica	x gas	x liquid	x vapour	heat capacity
0	0.5	0.25	0.15836	0.09164	1469.71
10	0.5	0.25	0.167191	0.082809	1536.65
20	0.5	0.25	0.176169	0.073831	1603.93
30	0.5	0.25	0.185202	0.064798	1671.34
40	0.5	0.25	0.194291	0.055709	1738.88
50	0.5	0.25	0.203437	0.046563	1806.55
60	0.5	0.25	0.212638	0.037362	1874.35
70	0.5	0.25	0.221894	0.028106	1942.27
80	0.5	0.25	0.231207	0.018793	2010.33
90	0.5	0.25	0.240576	0.009424	2078.51
100	0.5	0.25	0.25	0	2146.83

Table 35 : Variation in phase change at t_f = 323 K

Humidity	x silica	x gas	x liquid	x vapour	heat capacity
0	0.5	0.25	0.096246	0.153754	1344.333
10	0.5	0.25	0.110647	0.139353	1424.385
20	0.5	0.25	0.125261	0.124739	1504.93
30	0.5	0.25	0.140089	0.109911	1585.973
40	0.5	0.25	0.155132	0.094868	1667.515
50	0.5	0.25	0.170392	0.079608	1749.561
60	0.5	0.25	0.185871	0.064129	1832.114
70	0.5	0.25	0.20157	0.04843	1915.178
80	0.5	0.25	0.21749	0.03251	1998.755
90	0.5	0.25	0.233633	0.016367	2082.849
100	0.5	0.25	0.25	0	2167.464

Table 36: Variation in phase change at t_f = 348 K

Humidity	x silica	x gas	x liquid	x vapour	heat capacity
0	0.5	0.25	0	0.25	1138.492

10	0.5	0.25	0.049322	0.200678	1300.498
20	0.5	0.25	0.069574	0.180426	1394.606
30	0.5	0.25	0.09032	0.15968	1489.866
40	0.5	0.25	0.111567	0.138433	1586.296
50	0.5	0.25	0.133322	0.116678	1683.915
60	0.5	0.25	0.155594	0.094406	1782.739
70	0.5	0.25	0.17839	0.07161	1882.787
80	0.5	0.25	0.201717	0.048283	1984.078
90	0.5	0.25	0.225585	0.024415	2086.629
100	0.5	0.25	0.25	0	2190.46

Table 37 : Variation in phase change at t_f = 373 K

Figure 20 below shows the variation in specific heat capacity with humidity at the different temperatures.

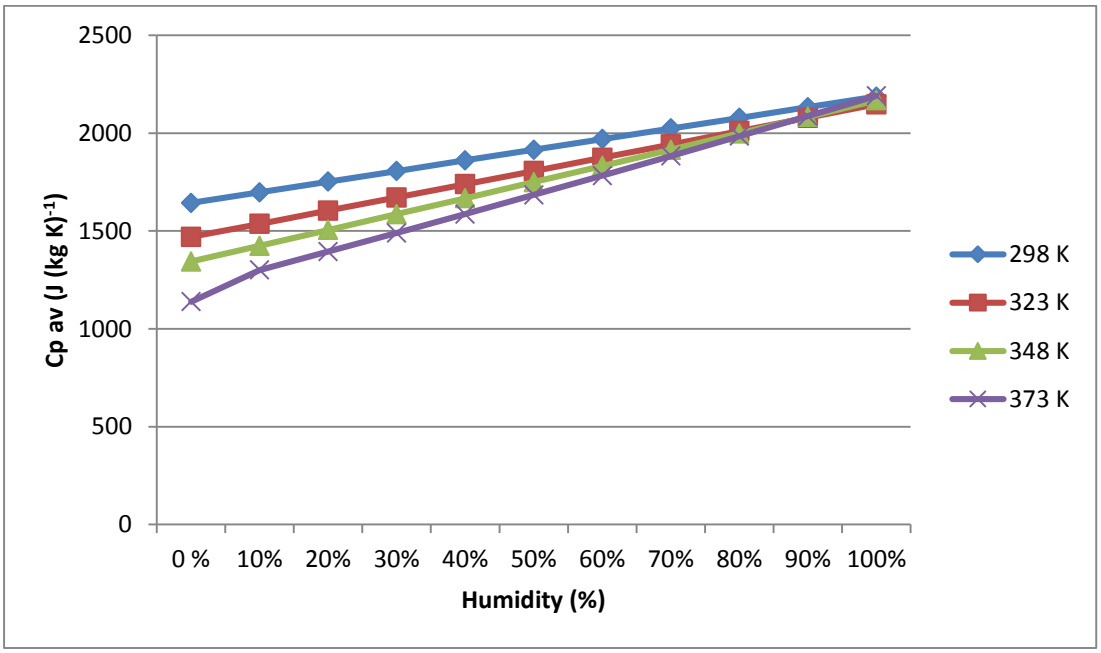

Figure 20

Table 38 below shows the variation in latent heat required by the liquid phase to transition into the vapour phase as the mass fraction of the vapour phase reduces with temperature.

latent heat (kJ)	298	323	348	373
0%	3059.136	8269.594	13874.76	22560
10%	2750.086	7472.672	12575.23	18109.22
20%	2445.504	6662.534	11256.48	16281.63
30%	2138.956	5847.356	9918.412	14409.52
40%	1833.391	5027.139	8560.901	12492.21
50%	1527.825	4201.881	7183.809	10529

60%	1222.26	3371.585	5787.004	8519.196
70%	916.6953	2536.248	4370.355	6462.103
80%	611.1302	1695.872	2933.726	4357.014
90%	305.5651	850.4557	1476.985	2203.218
100%	0	0	0	0

Table 38: Latent heat required

The variation in work done on the liquid as the mass fraction of the vapour phase decreases with an increase in humidity is shown below in Table 39.

work done	298 K	323 K	348 K	373 K
0%	1996.356	5396.639	9054.505	14722.39
10%	1794.673	4876.577	8206.444	11817.86
20%	1595.265	4347.891	7345.844	10625.2
30%	1395.857	3815.915	6472.639	9403.484
40%	1196.449	3280.651	5586.743	8152.267
50%	997.0408	2742.098	4688.068	6871.099
60%	797.6326	2200.256	3776.53	5559.527
70%	598.2245	1655.125	2852.042	4217.092
80%	398.8163	1106.706	1914.515	2843.336
90%	199.4082	554.9973	963.863	1437.794
100%	0	0	0	0

Table 39: Variation in work done due to humidity

Assuming no latent heat within the vapour phase, the heat required to raise the temperature of the soil model to the final temperatures is indicated below in Table 40.

Q (kJ)	T_f = 298 K	323 K	348 K	373 K
0%	985.9508	2455.658	3799.991	4938.482
10%	1018.606	2555.254	3979.638	5280.136
20%	1051.206	2655.135	4160.065	5253.566
30%	1083.807	2755.145	4341.118	5830.984
40%	1116.407	2855.285	4522.801	6109.097
50%	1149.008	2955.554	4705.116	6389.03
60%	1181.608	3055.953	4888.067	6670.806
70%	1214.209	3156.48	5071.658	6954.445
80%	1246.809	3257.137	5255.892	7239.97
90%	1279.41	3357.924	5440.773	7527.402
100%	1312.01	3458.839	5626.303	7816.763

Table 40: Heat required for temperature change within soil model

Therefore the sum of heats at the range of temperatures can be calculated by adding the heat required to the soil to the latent heat minus the heat lost as work is done over the phase change, Table 41.

Total Q required	298 K	323 K	348 K	373 K
0%	2048.731	5328.612	8620.247	12776.09
10%	1974.018	5151.348	8348.421	11571.49
20%	1901.445	4969.778	8070.699	11211.1
30%	1826.905	4786.586	7786.892	10837.02
40%	1753.349	4601.773	7496.959	10449.04
50%	1679.792	4415.338	7200.856	10046.93
60%	1606.236	4227.281	6898.541	9630.476
70%	1532.68	4037.603	6589.971	9199.457
80%	1459.123	3846.303	6275.103	8753.648
90%	1385.567	3653.382	5953.895	8292.826
100%	1312.01	3458.839	5626.303	7816.763

Table 41: Total heat required as a function of humidity

Appendix F.2

Table 43 below indicates the entropy of vaporization as a result of the calculated phase change in F.1. The ΔS_{vap} = 108.951 J mol^{-1} K^{-1}.

S vap	298	323	348	373
0 %	8.207642	22.18727	37.22589	60.52833
10 %	7.378462	20.04913	33.73925	48.58692
20 %	6.558633	17.87553	30.20105	43.68351
30 %	5.738804	15.68842	26.61104	38.66066
40 %	4.918975	13.48778	22.96884	33.51651
50 %	4.099146	11.27362	19.27411	28.24923
60 %	3.279317	9.045939	15.52649	22.85695
70 %	2.459487	6.804737	11.72563	17.33778
80 %	1.639658	4.550013	7.871167	11.68984
90 %	0.819829	2.281767	3.962741	5.911219
100 %	0	0	0	0

Table 42: Variation in entropy of vaporization due to humidity

The total entropy change was then calculated as a function of the total heat added to the system added to the total entropy of vaporization as the phase change within the soil from the liquid to the vapour phase occurred, Table 43.

Entropy Change	298 K	323 K	348 K	373 K
0%	15.08258	38.68452	61.99672	94.78059
10%	14.00268	35.99758	57.72897	79.60969
20%	12.93932	33.26184	53.39272	73.74009
30%	11.86936	30.50757	48.98716	67.71434
40%	10.8027	27.73475	44.51183	61.53002
50%	9.736033	24.9434	39.96623	55.1847

60%	8.66937	22.1335	35.34989	48.67592
70%	7.602707	19.30506	30.66233	42.0012
80%	6.536045	16.45807	25.90307	35.15807
90%	5.469382	13.59255	21.07163	28.144
100%	4.402719	10.70848	16.16754	20.95647

Table 43 : Variation in Entropy change within temperature

Appendix F.3

Table 44 below indicates the variation in specific heat capacity of air (cv) as humidity increases and the vapour component within the air increases.

cv air	298	323	348	373
0	718	718	718	718
10	857.8346	858.2496	858.7597	859.3632
20	997.6692	998.4992	999.5194	1000.726
30	1137.504	1138.749	1140.279	1142.089
40	1277.338	1278.998	1281.039	1283.453
50	1417.173	1419.248	1421.798	1424.816
60	1557.008	1559.498	1562.558	1566.179
70	1696.842	1699.747	1703.318	1707.542
80	1836.677	1839.997	1844.078	1848.905
90	1976.511	1980.246	1984.837	1990.268
100	2116.346	2120.496	2125.597	2131.632

Table 44: Variation in c_v air with humidity

Tables 45 to 48 indicate the variation in specific heat capacity (c_v) of the soil based on the phase change previously calculated as a function of increasing humidity.

Humidity	x silica	x gas	x liquid	x vapour	Average Heat
0	0.5	0.25	0.2161	0.0339	1489.193
10	0.5	0.25	0.219525	0.030475	1533.527
20	0.5	0.25	0.222911	0.027089	1577.756
30	0.5	0.25	0.226297	0.023703	1621.984
40	0.5	0.25	0.229683	0.020317	1666.213
50	0.5	0.25	0.233069	0.016931	1710.442
60	0.5	0.25	0.236455	0.013545	1754.671
70	0.5	0.25	0.239842	0.010158	1798.899
80	0.5	0.25	0.243228	0.006772	1843.128
90	0.5	0.25	0.246614	0.003386	1887.357
100	0.5	0.25	0.25	0	1931.586

Table 45: Variation in c_v soil model at 298 K

Humidity	x silica	x gas	x liquid	x vapour	heat required
0	0.5	0.25	0.15836	0.09164	1331.394
10	0.5	0.25	0.167191	0.082809	1389.643
20	0.5	0.25	0.176169	0.073831	1448.277
30	0.5	0.25	0.185202	0.064798	1507.058
40	0.5	0.25	0.194291	0.055709	1565.985
50	0.5	0.25	0.203437	0.046563	1625.059
60	0.5	0.25	0.212638	0.037362	1684.279
70	0.5	0.25	0.221894	0.028106	1743.647
80	0.5	0.25	0.231207	0.018793	1803.16
90	0.5	0.25	0.240576	0.009424	1862.821
100	0.5	0.25	0.25	0	1922.628

Table 46: Variation in c_v soil model at 323 K

Humidity	x silica	x gas	x liquid	x vapour	heat required
0	0.5	0.25	0.096246	0.153754	1158.004
10	0.5	0.25	0.110647	0.139353	1229.272
20	0.5	0.25	0.125261	0.124739	1301.074
30	0.5	0.25	0.140089	0.109911	1373.412
40	0.5	0.25	0.155132	0.094868	1446.29
50	0.5	0.25	0.170392	0.079608	1519.712
60	0.5	0.25	0.185871	0.064129	1593.681
70	0.5	0.25	0.20157	0.04843	1668.201
80	0.5	0.25	0.21749	0.03251	1743.275
90	0.5	0.25	0.233633	0.016367	1818.908
100	0.5	0.25	0.25	0	1895.103

Table 47: Variation in c_v soil model at 348 K

Humidity	x silica	x gas	x liquid	x vapour	heat capacity with air variation
0	0.5	0.25	0	0.25	918.3869
10	0.5	0.25	0.049322	0.200678	1072.137
20	0.5	0.25	0.069574	0.180426	1156.1
30	0.5	0.25	0.09032	0.15968	1241.247
40	0.5	0.25	0.111567	0.138433	1327.596
50	0.5	0.25	0.133322	0.116678	1415.167
60	0.5	0.25	0.155594	0.094406	1503.977

70	0.5	0.25	0.17839	0.07161	1594.045
80	0.5	0.25	0.201717	0.048283	1685.39
90	0.5	0.25	0.225585	0.024415	1778.031
100	0.5	0.25	0.25	0	1871.987

Table 48: Variation in c_v soil model at 373 K

Figure 21 provides a summary in the variation of average c_v within the soil model as humidity increases. The peak of the chart at 100 % is clearly visible as phase change reduces.

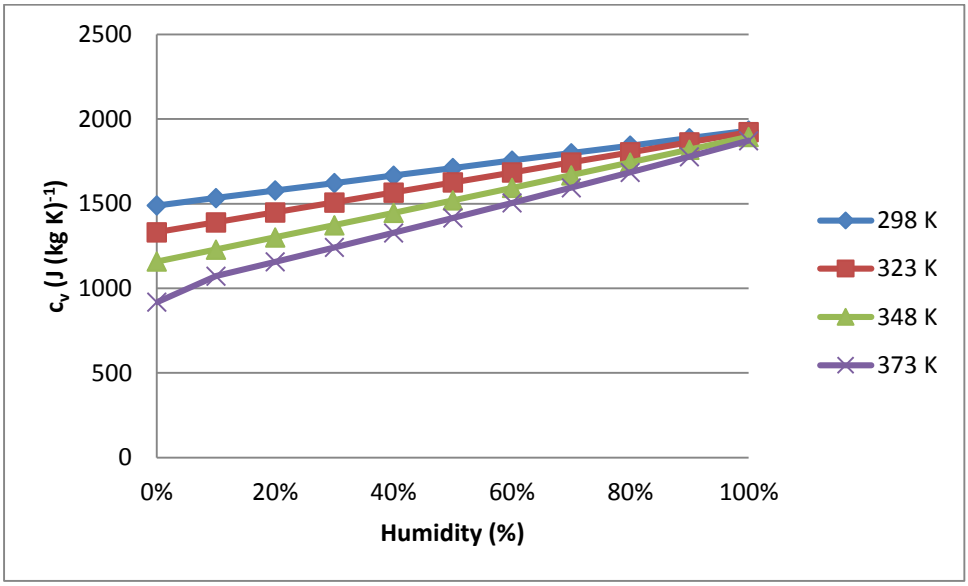

Figure 21: Variation in c_v as a function of humidity

The latent heat of vaporization, as well as the work done on the soil model were equal to the values indicated in Table 38 and 39 (Appendix F.1) Table 50 below indicates the total calculated change in internal energy across the temperature range as a function of increasing humidity.

dU	298 K	323 K	348 K	373 K
0	2551.973	5003.185	7831.066	11143.8
10 %	2488.939	4819.524	7564.89	10151.05
20 %	2427.011	4631.886	7293.426	9818.391
30 %	2365.083	4442.733	7016.646	9474.527
40 %	2303.155	4252.064	6734.513	9119.287
50 %	2241.227	4059.878	6446.991	8752.499
60 %	2179.298	3866.176	6154.044	8373.986
70 %	2117.37	3670.957	5855.635	7983.573
80 %	2055.442	3474.223	5551.727	7581.083
90 %	1993.514	3275.972	5242.284	7166.336
100 %	1931.586	3076.205	4927.268	6739.153

Table 49 : Variation in Internal Energy of the soil based on humidity